



Electron multipacting with long bunched proton beam

— *Theory and Simulation*

L. Wang, BNL

In collaboration with J. Wei, M. Blaskiewicz, P. He, Y.Y Lee, D. Raparia, S.Y. Zhang, N. Malitsky(BNL), R. Macek (LANL), K. Ohmi (KEK), F. Zimmermann (CERN), A. Chao (SLAC)

OUTLINE



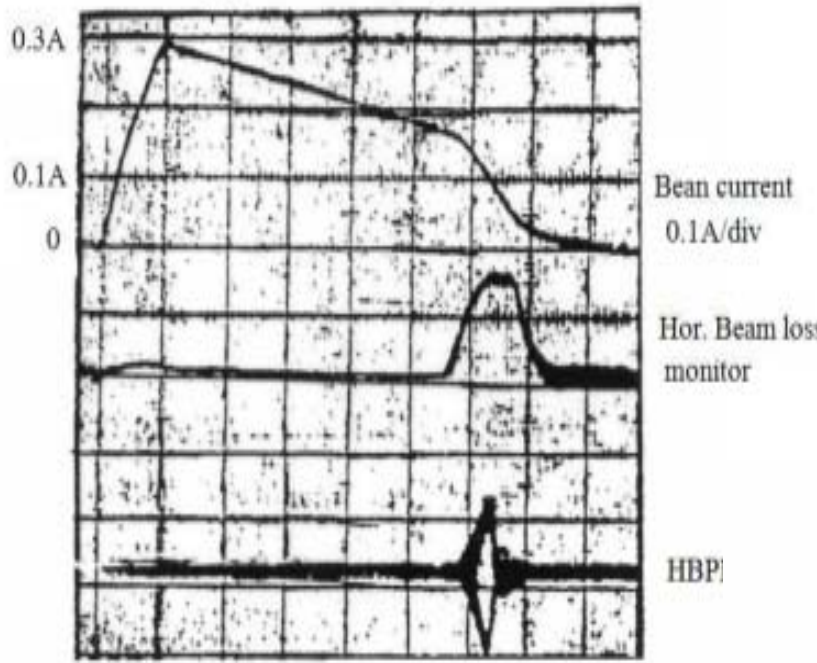
- Motivation
- Electron motion & Mechanism of multipacting
- Important factors related to Multipacting
 - Longitudinal beam profile
 - Transverse beam shape & size
 - Beam intensity
 - Peak SEY and Energy at Peak SEY
 -
- Multipacting in dipole Quadrupole & Sextupole magnets
- Electron cloud clearing with solenoids & clearing electrodes
- Summary

Overview

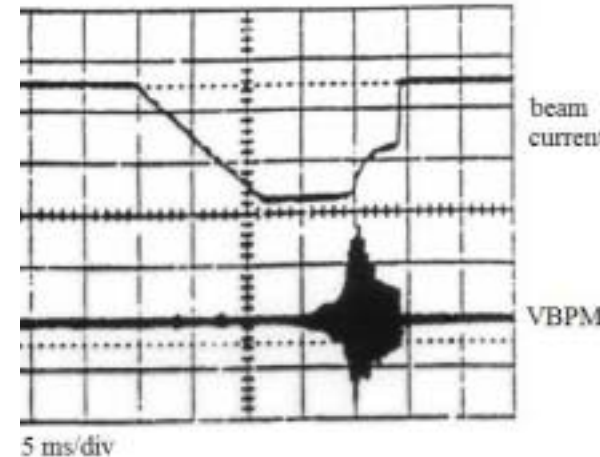


- 1965 INP PSR transverse instability & beam loss
- 1971 ISR e-p, 1977 beam-induced multipacting
- 1988 LANL PSR vertical instability & beam loss
- 1989 KEK PF vertical coupled bunch instability(CBI)
- since 1996 BEPC IHEP-KEK collaboration(CBI)
- 1997 LHC crash program launched at CERN
- 1997 CESR trapped ecloud causes coupled bunch instability
- 1997/98 APS e-cloud studies start
- since 1998 SPS e. cloud with LHC beam
- 2000 PS e-cloud with LHC beam (Heating & instability)
- Since 1999 e-cloud at KEKB and PEP-II (blow-up, pressure rise, tune shift along the train, CBI, luminosity drop...)
- Since October 2001 evidence for e-cloud at RHIC (Vacuum pressure...)
- Observation of secondary particles in the booster proton beam are presented in the Booster E-Log at 04/06/01, Tevatron...

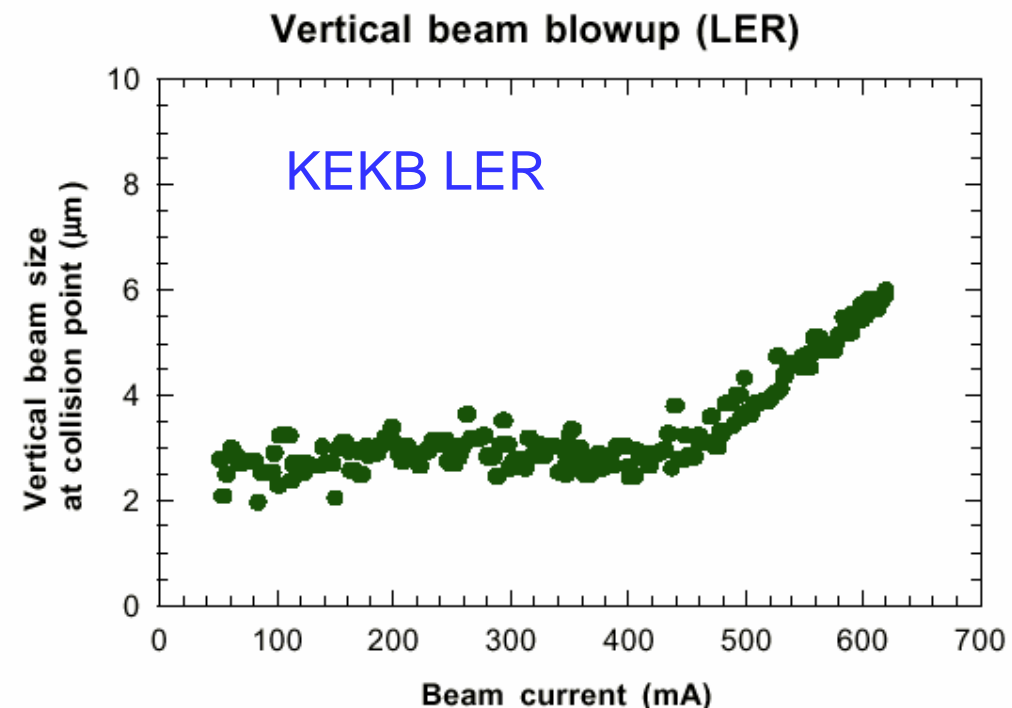
Transverse instability in the two PSR & beam size blow-up in KEKB



*Transverse instability in the
INP PSR
bunched beam (1965)*



*Transverse
instability in Los
Alamos PSR,
bunched beam
(1986)*



Motivation



- What is the mechanism of trailing edge multipacting?
- Which factors affect e-cloud multipacting?
And How?
- How to Clear electron cloud?

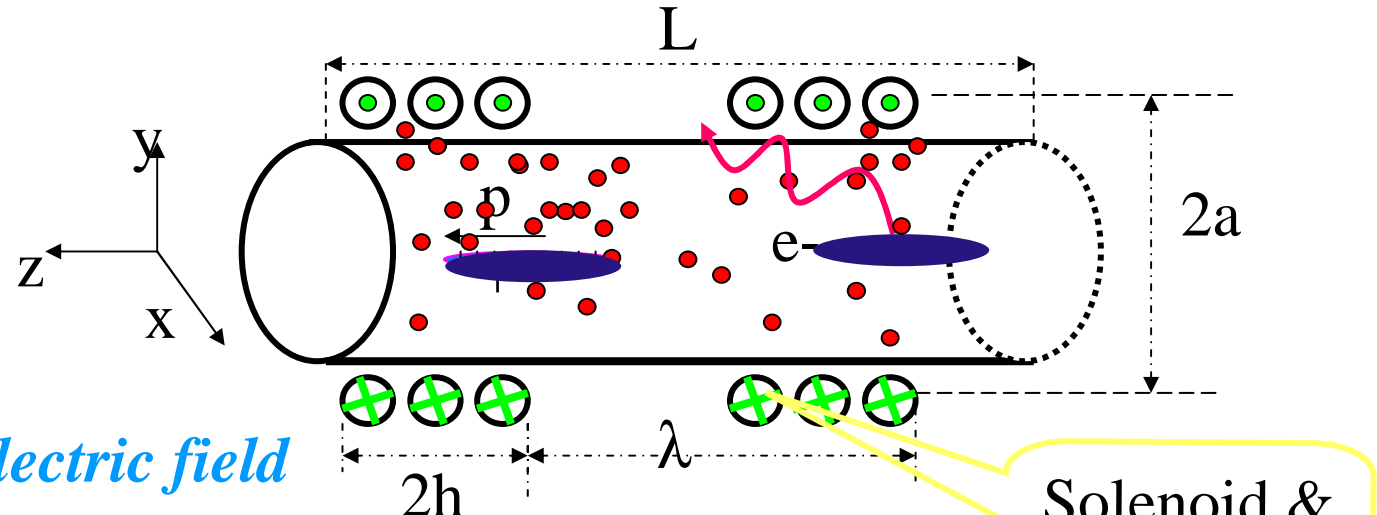
3D PIC Program--- CLOUDLAND



CLOUDLAND is a complete 3D PIC code for e-cloud initially developed for KEKB (*PRST-AB 124402*)

Program model

- ◆ PIC methods



Magnetic and electric field

- ◆ General 3-dimensional fields given by expression.
- ◆ Fields can also be import from other program using table

Beam potential

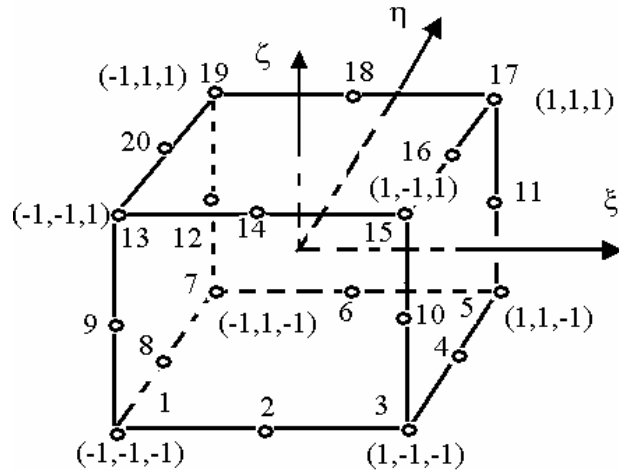
- ◆ Gaussian bunch in round chamber (image charge is included)
- ◆ PIC method for general geometry

Secondary emission and reflective electron are included

Particle Mesh technique applied in the Space charge potential solver



- Three dimensional **irregular mesh** to better represent the general chamber geometry
- handle accuracy with **high order elements**.



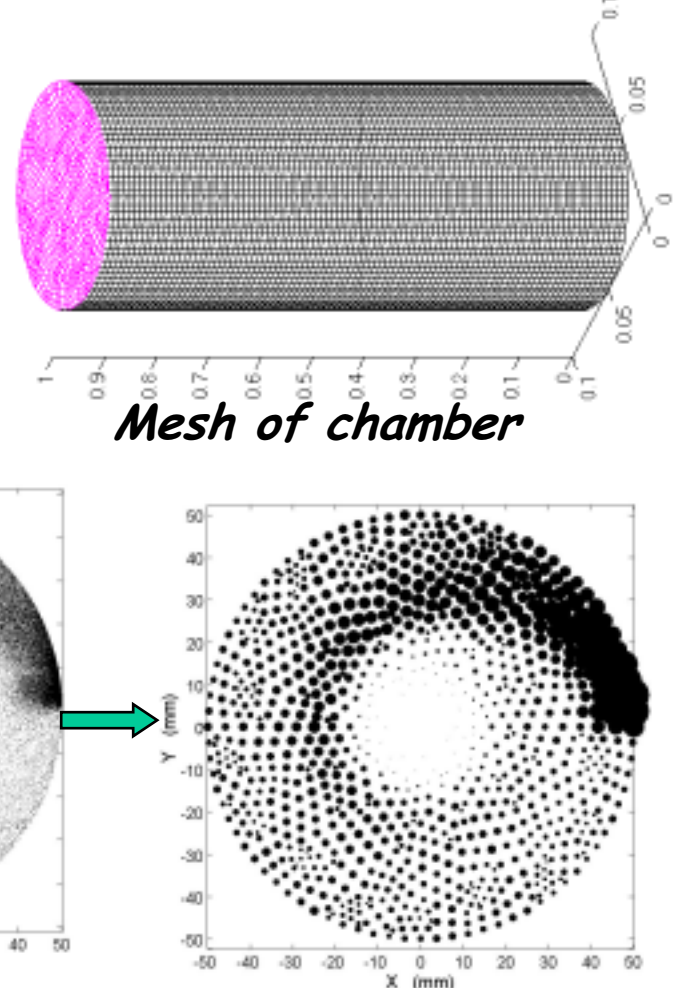
20 node element

Charge assignment

$$Q_i = N_i Q_0 \quad \sum_i N_i = 1$$

Real charge distribution

Meshed Charge distribution

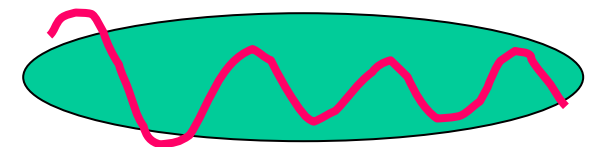


Classification of electron multipacting



If an electron can oscillate many times under the beam force during the passage of one bunch, then the bunch is called long bunch

$$\frac{\hat{z}\bar{\omega}}{\pi\beta c} \gg 1$$



Long bunch (Single bunch multipacting): PSR, SNS, JPAC, ISIS, ESS...

Short bunch (Multibunch multipacting): B-factories, PF, NLC damping ring, SPS, LHC, RHIC,.....

Source of electrons



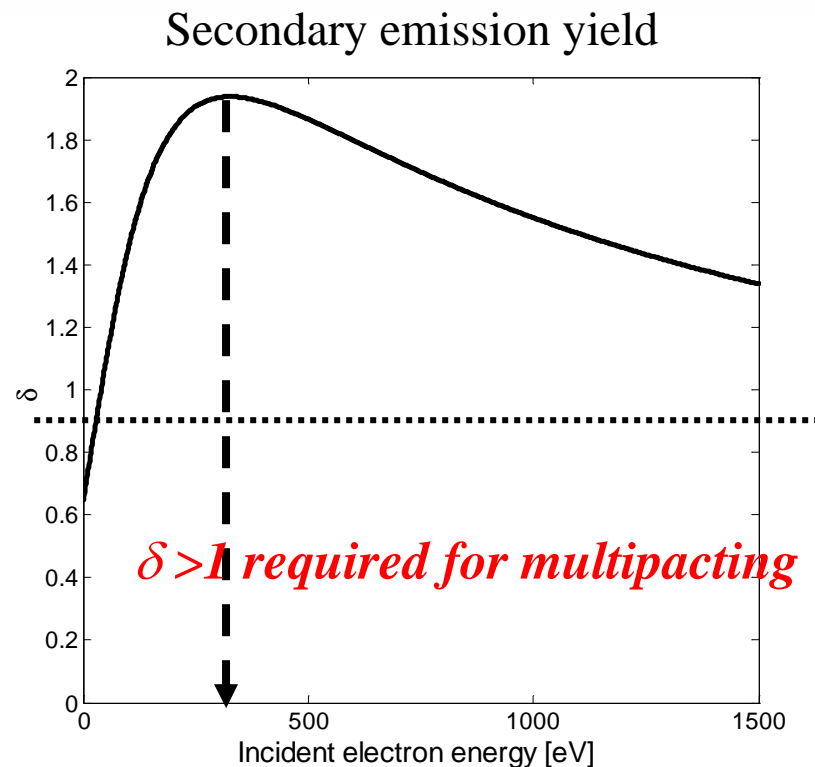
Primary electrons

- **Photon-electrons**
(electron machine & LHC)
- **Beam loss** at the chamber surface (PSR, SNS, ISIS, ESS, JPARC)
- Residual **gas ionization**
- **Stripped electrons**
-

Table 1 Parameters for the SNS

Parameter	Description	SNS
E (GeV)	Beam energy	1.9
C (m)	Circumference	248
N_p	Beam intensity	2.05×10^{14}
a_x, a_y (mm)	Transverse beam size	28, 28
τ_b (ns)	Bunch length	700
b (cm)	Beam pipe radius	10
P_l	Proton loss rate/turn	1.1×10^{-6}
Y	Assumed proton-electron yield	100

Secondary electrons



Key parameters for Multipacting (Strong **energy** and **SEY** dependence)

- SEY depend on the material property of the chamber surface (peak SEY and energy at peak SEY)
- Beam-electron interaction dependence (beam pattern, bunch current, bunch shape, bunch length, chamber size...)

Beam space charge field



SNS beam transverse profile shape

- **Square shape** resulting from correlated painting during the injection.
- Inclusion of the space charge causes rapid diffusion in azimuthal direction and results in **round beam shape**
- **Electron Multipacting (energy at the wall surface)** **does not depend on transverse profile**

Space charge field of uniform cylinder beam

$$E_r(r,t) = \begin{cases} \frac{\lambda(t)}{4\pi\epsilon_0} \frac{2}{r} & (r > a) \\ \frac{\lambda(t)}{4\pi\epsilon_0} \frac{2r}{a^2} & (r < a) \end{cases}$$
$$U(r,t) = \begin{cases} \frac{\lambda(t)}{4\pi\epsilon_0} \left(1 + 2 \ln \frac{r}{a} \right) & (r > a) \\ \frac{\lambda(t)}{4\pi\epsilon_0} \frac{r^2}{a^2} & (r < a) \end{cases}$$

Nonlinear Hamiltonian of the radial motion

$$H = \frac{p^2}{2m} + eU(r,t)$$

The longitudinal beam force is neglected

Nonlinear Oscillation Period and Adiabatic invariant



Nonlinear Oscillation Frequency

$$T = 4.0 \int_0^{r_{amp}} \frac{dr}{v(r)} = 4.0 \int_0^{r_{amp}} \frac{dr}{\sqrt{2\Phi e / m}}$$

$$T = \begin{cases} 4.0 \sqrt{\frac{\pi \epsilon_0 m}{\lambda e}} \left(\sqrt{2a} \arcsin \frac{1}{\sqrt{1+2\ln(r_{amp}/a)}} + \int_a^{r_{amp}} \frac{dr}{\sqrt{\ln(r_{amp}/r)}} \right) \\ 2\pi a \sqrt{\frac{2\pi \epsilon_0 m}{\lambda e}} & (r_{amp} \leq a) \end{cases}$$

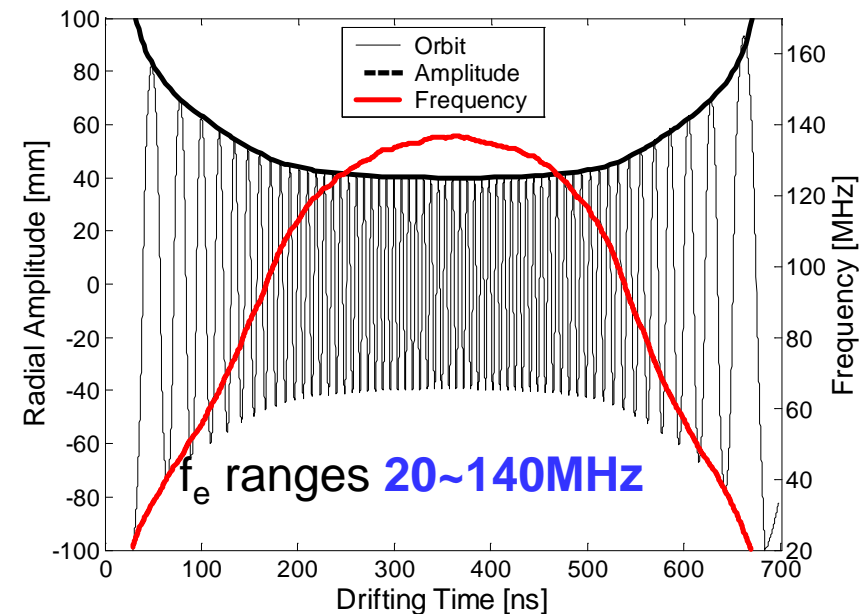
Adiabatic invariant

$$\frac{1}{\omega_e^2} \frac{d\omega_e}{dt} \ll 1 \quad (\text{if } t > 20\text{ns and } t < 680\text{ns for SNS})$$

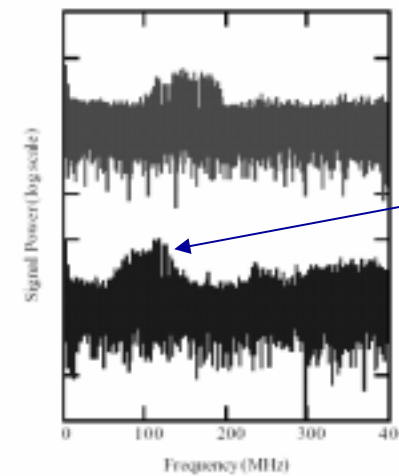
$$J = \oint pdq$$

$$J = \begin{cases} \frac{\pi r_{amp}^2}{a} \sqrt{\frac{me\lambda}{2\pi\epsilon_0}} & (r_{amp} < a) \\ 4a \sqrt{\frac{me\lambda}{2\pi\epsilon_0}} \left(\frac{\sqrt{2}}{2} x^{1/2} + \frac{1+2x}{2} \operatorname{arctg} \frac{1}{\sqrt{2x}} + \frac{\sqrt{2}}{a} \int_a^{r_{amp}} \sqrt{\ln \frac{r_{amp}}{r}} dr \right) & (r_{amp} > a) \end{cases}$$

$x = \ln(r_{amp}/a)$



Oscillation amplitude and frequency

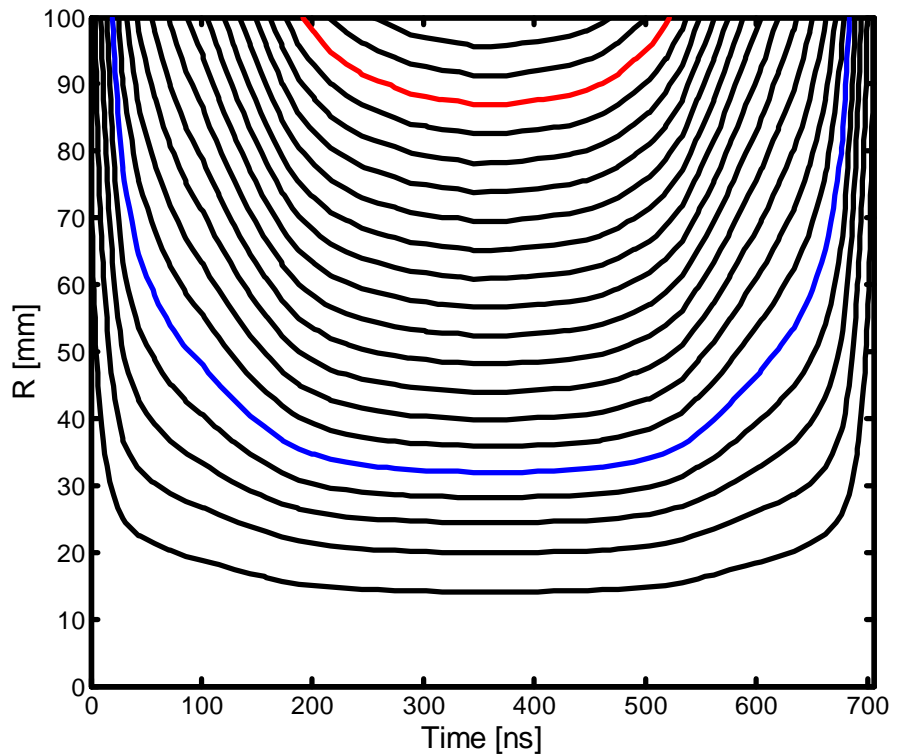


LANL PSR
beam spectrum
50~150MHz
courtesy
Robert J. Macek

Oscillation amplitude from adiabatic invariant



- Contour plot from adiabatic invariant can clearly describe the electron orbit
- All electrons emitted (including gas ionization) before the bunch center or survived from last bunch gap can be trapped (inside beam for the survived electrons) during the bunch passage and are released at the bunch tail. The trapped electrons, most of them are the survived electrons from the last bunch gap, contribute to beam dynamics (instabilities)
- All electrons which emitted from the wall after bunch center will directly drift to the opposite of wall surface. The straight drifting electrons contribute to multipacting due to their short drifting time & high energy when they hit the wall surface.

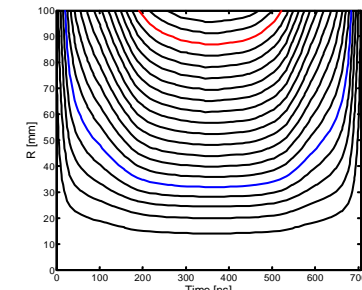
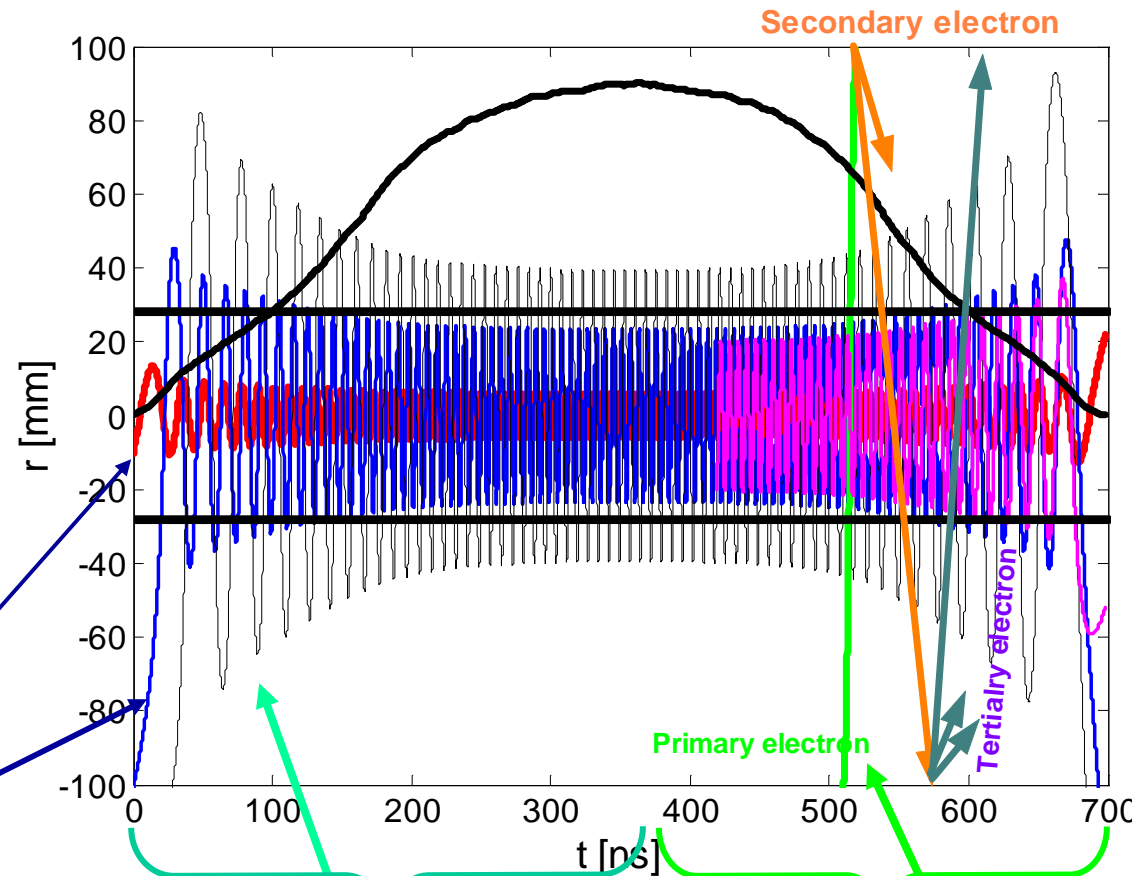


Contour plot of the oscillation amplitude resulting from adiabatic invariant for SNS beam

Particle motion vs. instability & multipacting



Typical orbits of various electrons trapped by SNS beam, bold solid line shows the longitudinal beam profile shape and the dashed back lines show the beam size



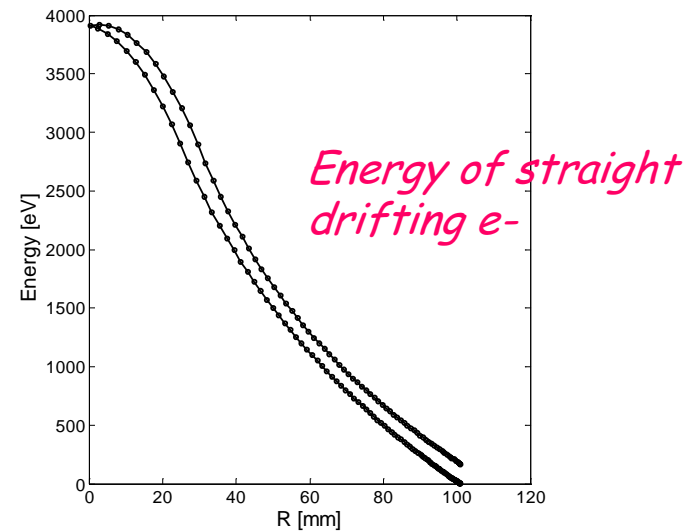
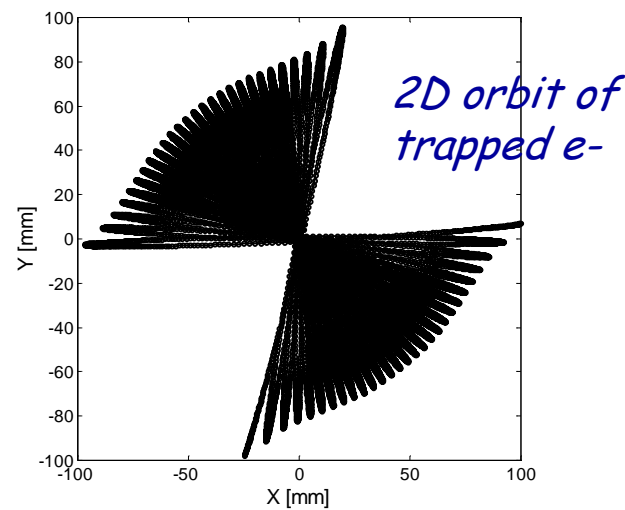
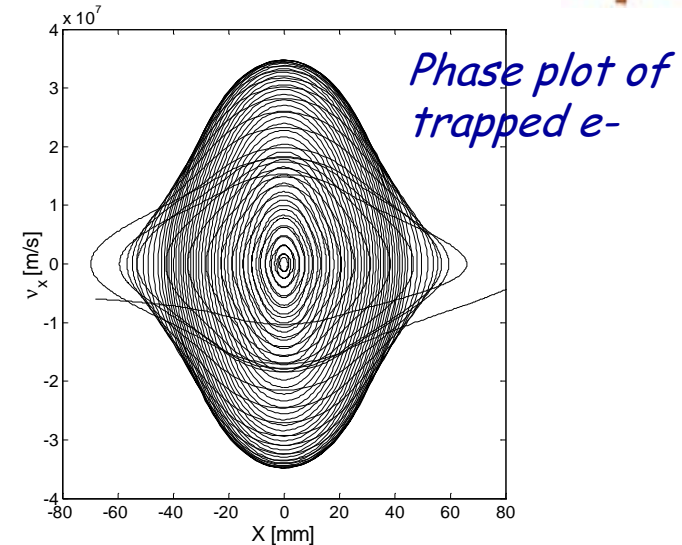
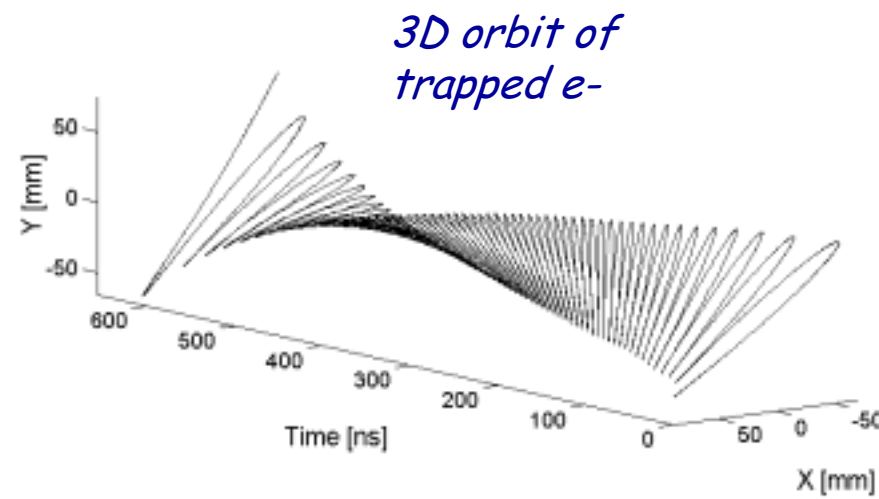
Electrons survived from the bunch gap (beam instabilities)

Electrons emitted before bunch center (trapped and lost after bunch center, multipacting)

Electrons emitted after the bunch center (multipacting)

**Electrons by ionization
(beam instabilities)**

Samples of orbit, phase plot, energy



Energy Gain of straight drifting electron & Mechanism of trailing edge multipacting



Assuming the beam line density is a linear function of time during the short electron drifting time($\sim 10\text{ns}$)

$$\Delta\lambda \approx \frac{\partial\lambda}{\partial t} \Delta t = \frac{\partial\lambda}{\partial z} c\beta\Delta t$$

$$\Delta E = -\frac{1}{2} \sqrt{\frac{me}{2\pi\varepsilon_0}} \beta c \left(a(2\zeta - 1) \arcsin \frac{1}{\sqrt{\zeta}} + a \sqrt{2 \ln \frac{b}{a}} + \sqrt{2}\zeta \int_a^b \frac{dr}{\sqrt{\ln(b/r)}} - \frac{1}{\sqrt{2}} \int_a^b \frac{1 + 2 \ln(r/a)}{\sqrt{\ln(b/r)}} dr \right) \frac{\partial\lambda}{\partial z} \frac{1}{\sqrt{\lambda}}$$

$$\zeta = 1 + 2 \ln(b/a)$$

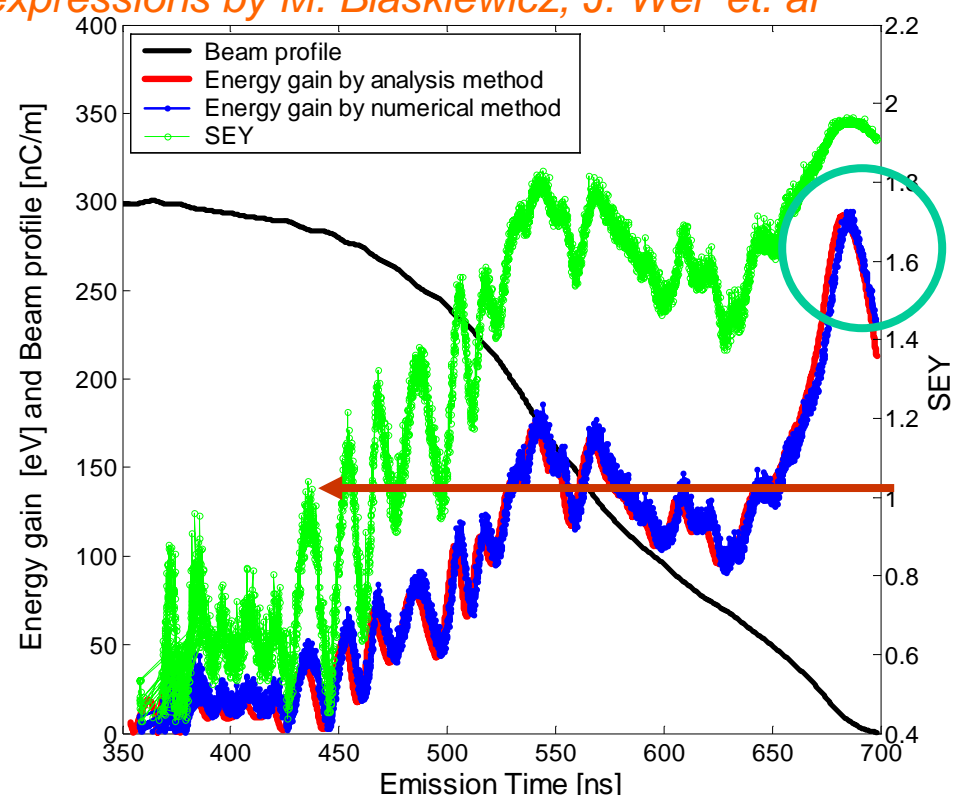
Also see other expressions by M. Blaskiewicz, J. Wei et. al

a : beam size, b , chamber radius, λ is beam line density

Longitudinal beam profile factor

$$Factor_{profile} = -\frac{\partial\lambda}{\partial z} \frac{1}{\sqrt{\lambda}}$$

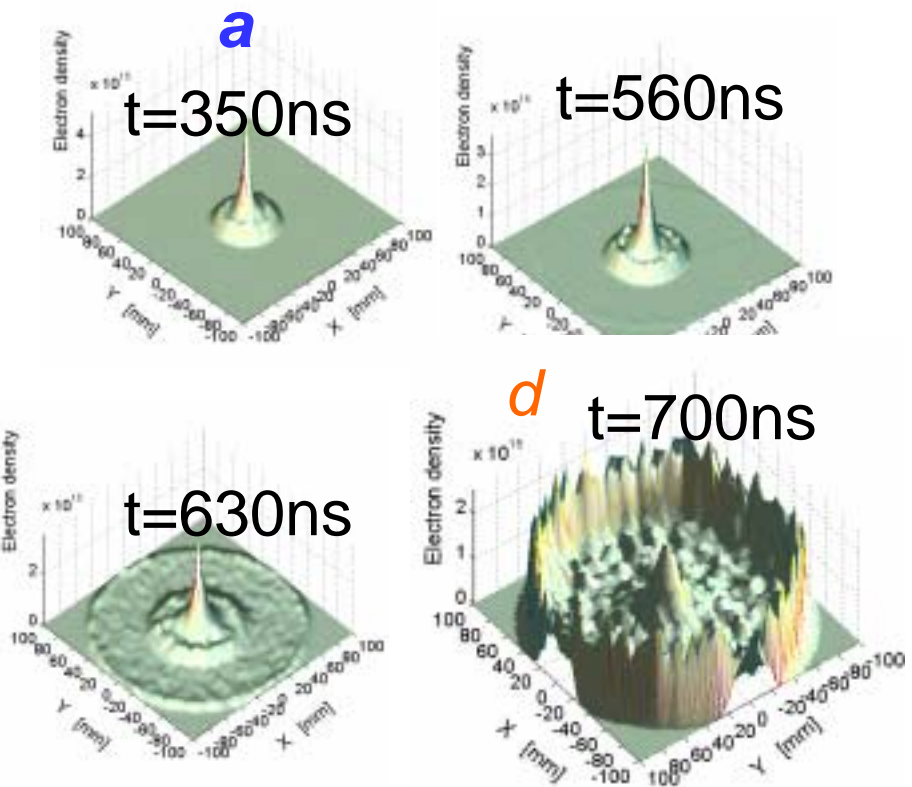
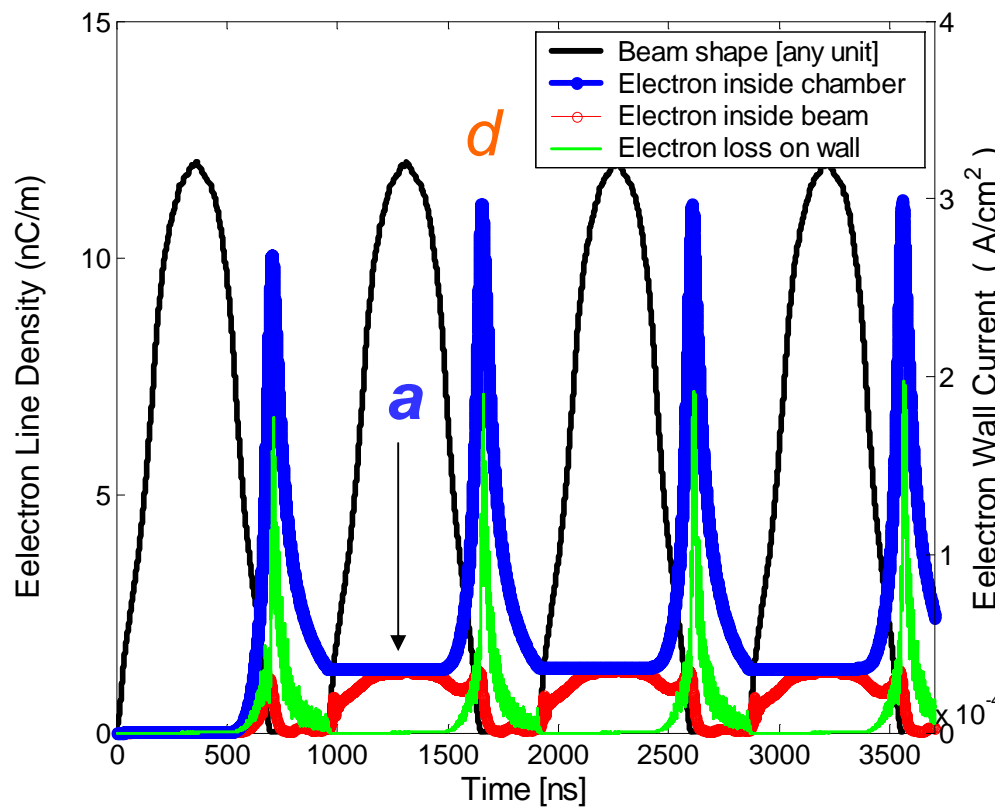
- Good agreement with numerical method
- Calculated SEY can be used to predict the multipacting directly
- Adiabatic motion and Energy gain can explain the mechanism of "trailing edge multipactor"



E-cloud in drift region



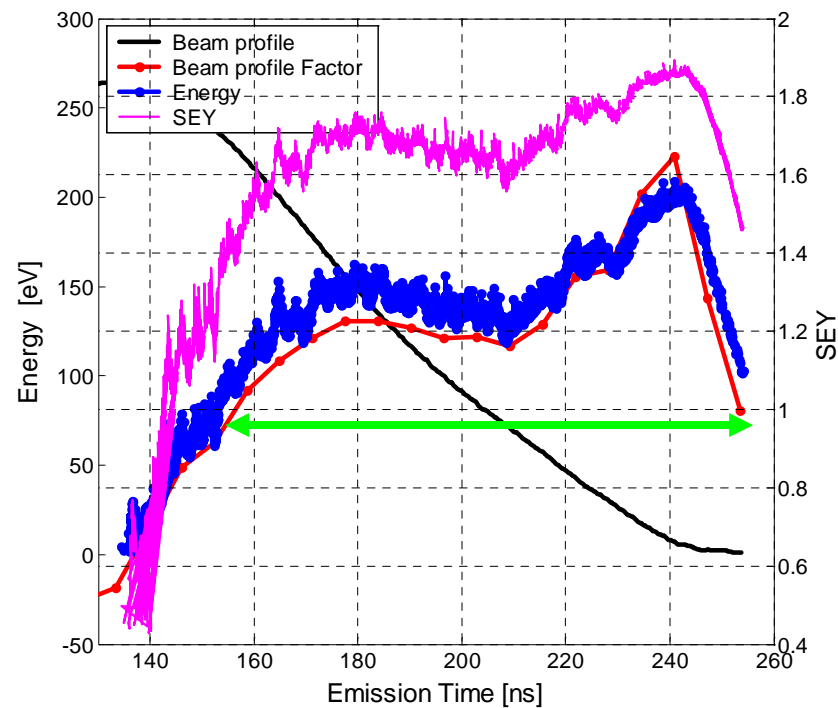
- Single bunch multipacting & Trailing Edge Multipacting
- All surviving electron from the last gap are trapped inside beam during the bunch passage (Contributing to beam instabilities)
- Bunch gap is important for *beam dynamics*



E-cloud build-up in SNS drift region

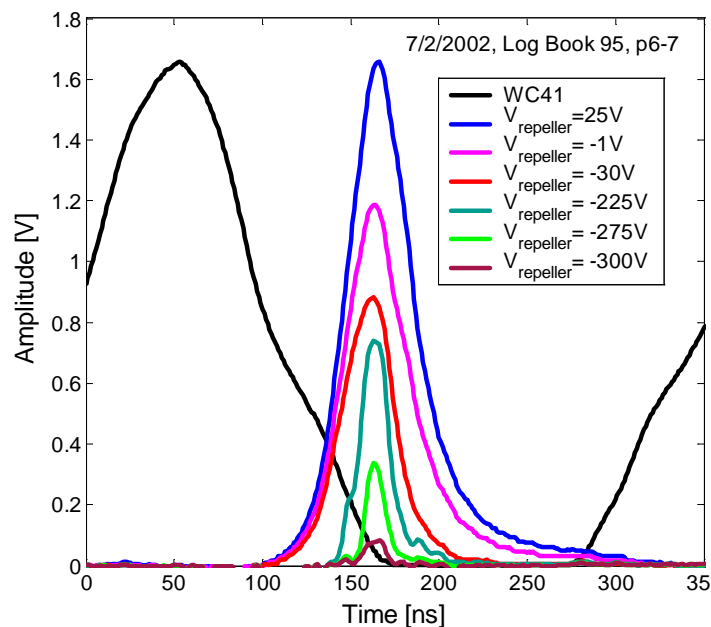
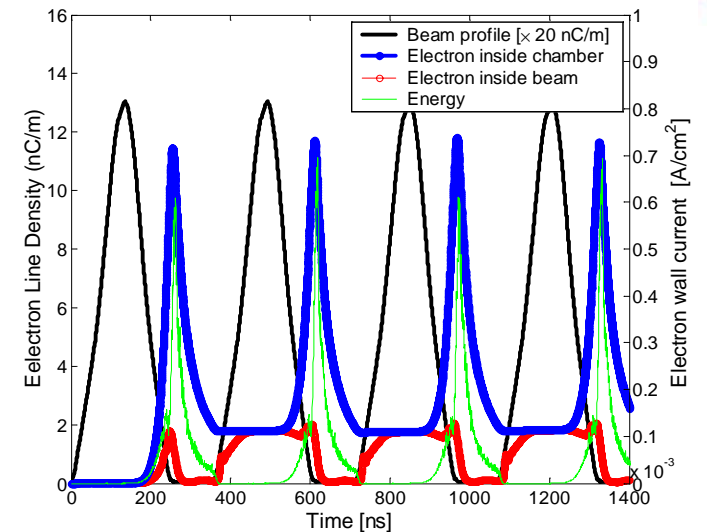
E-cloud distribution in different time

Ecloud in PSR



ED42Y Signals for various repeller voltages

courtesy Robert
J. Macek



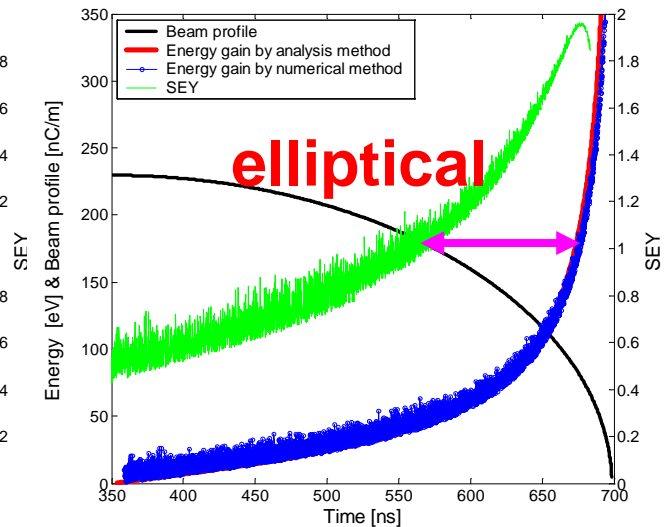
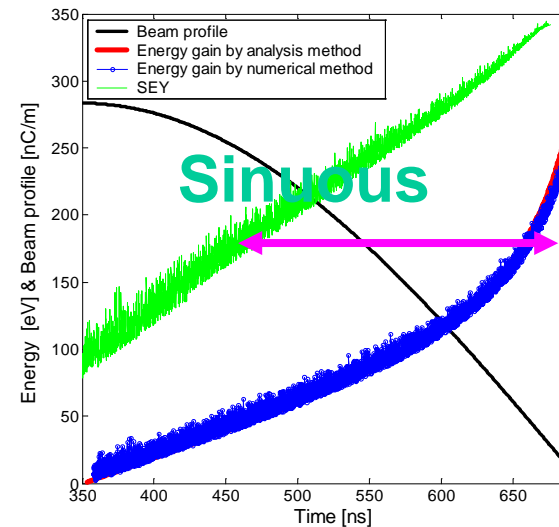
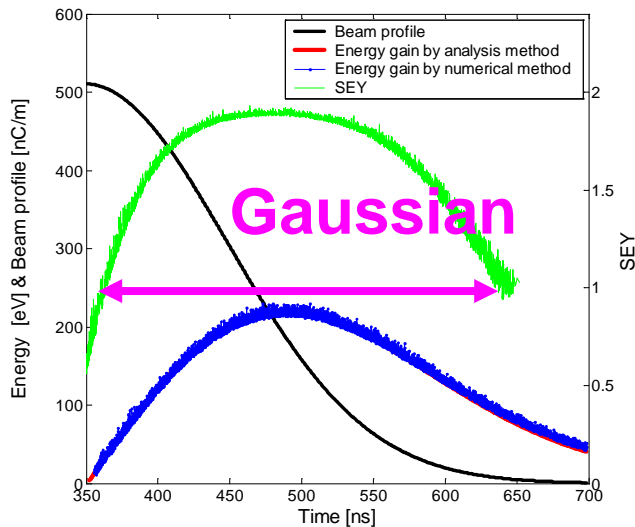
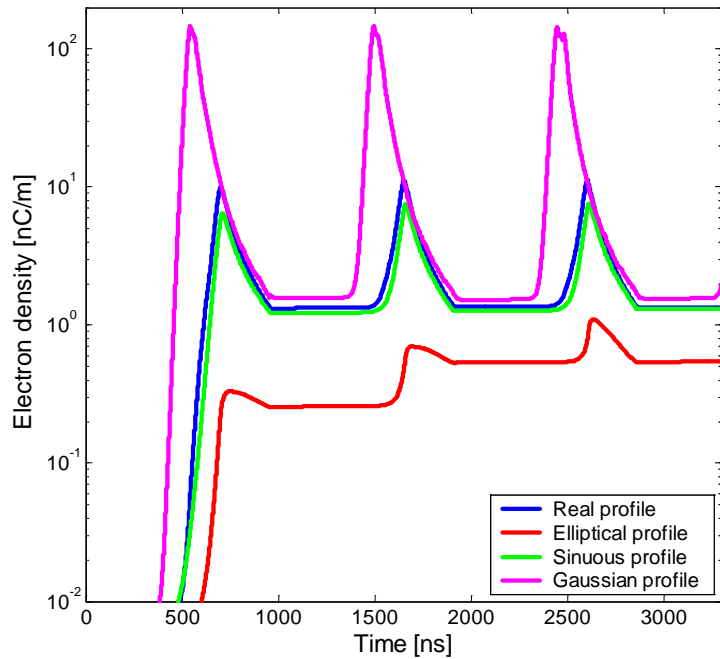
Important Factors Related to Electron multipacting(1)



Longitudinal Beam Profile

For assumed Gaussian, sinuous & elliptical beam profile:

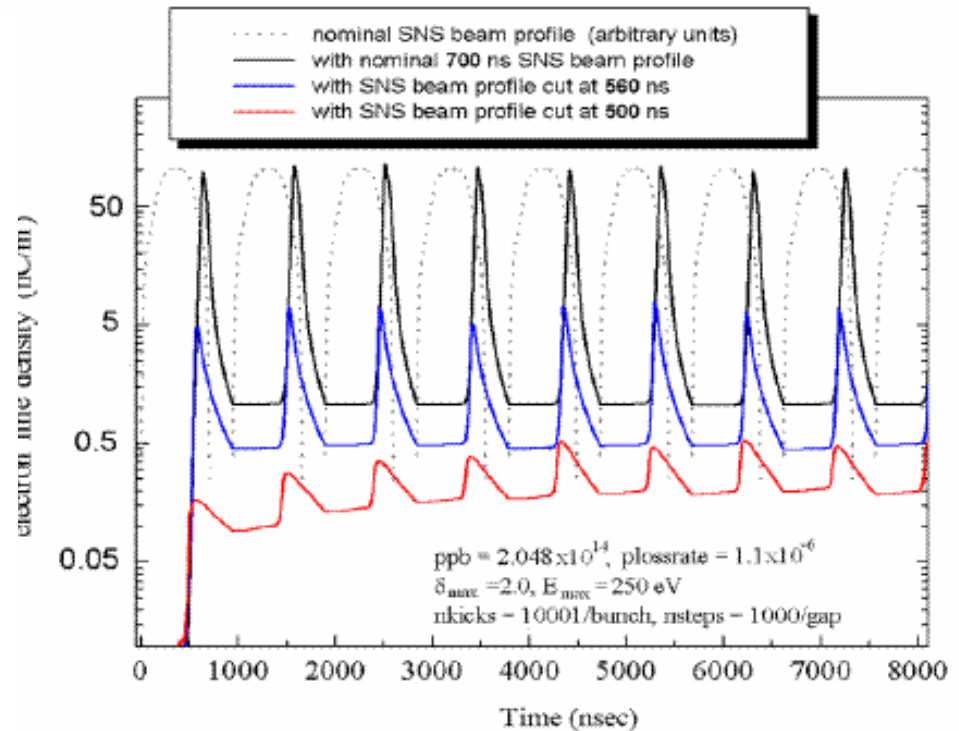
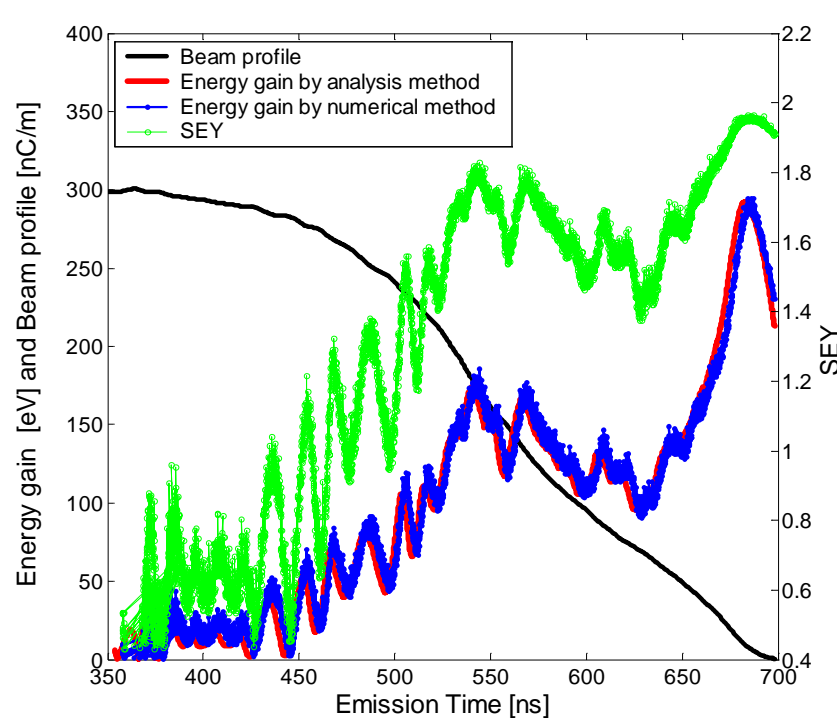
- Gaussian profile excites the strongest multipacting due to long bunch tail
- Elliptical profile has the weakest multipacting
- Electron cloud of the real profile is close to that of the sinuous profile



Longitudinal Profile effect, simulation



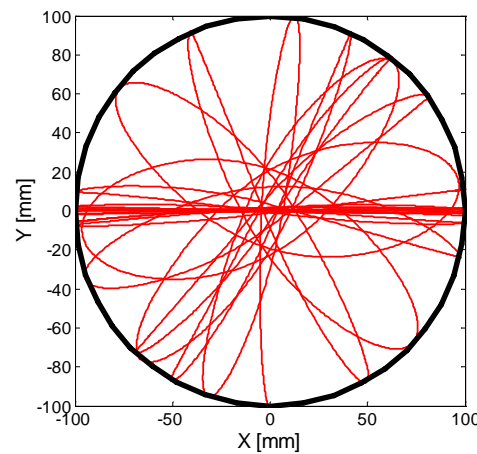
M.T. F. Pivi and M. A. Furman
PRSTAB Vol. 6, 034201 (2003))



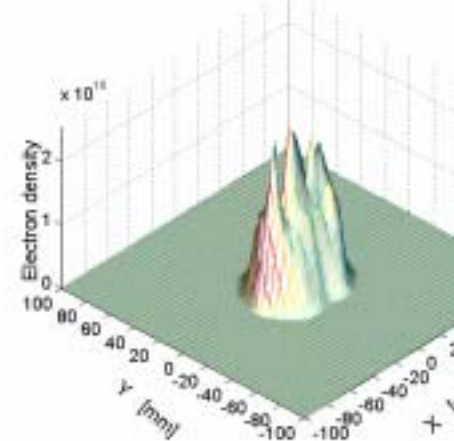
Flat beam effect on EC distribution



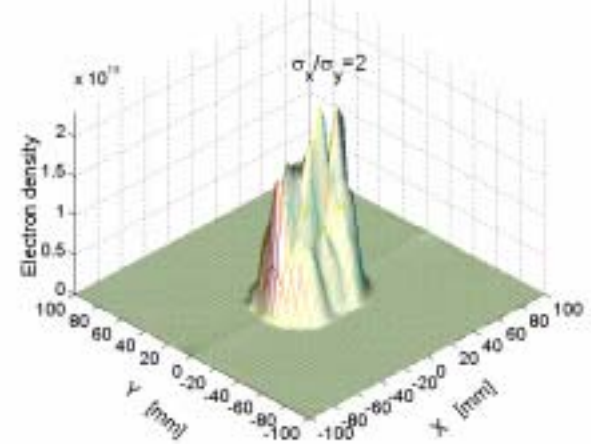
- Flat beam $\sigma_x : \sigma_y = 2:1$
- Stronger multipacting in larger beam size direction due to the “polarization effect” of strong beam space charge force



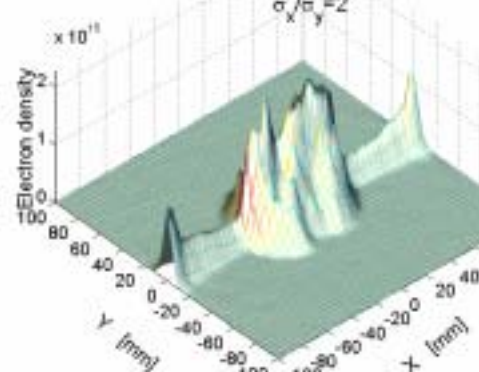
t=350ns



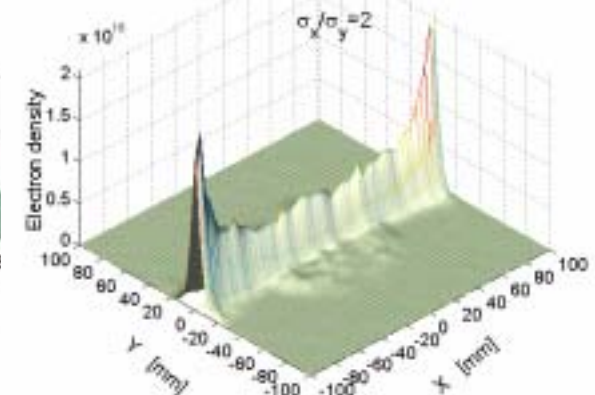
t=490ns



t=560ns



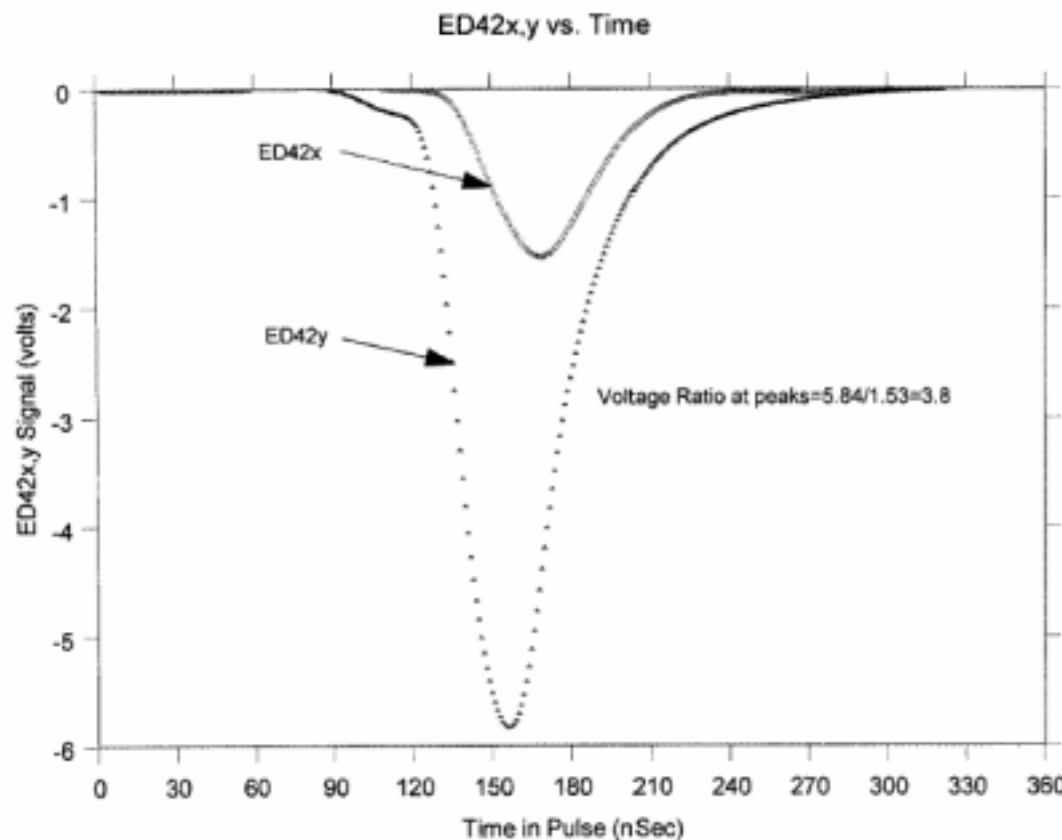
t=630ns



PSR experimental study----flat beam



- Qualitatively agrees with LANL PSR observation
- Instability & detector



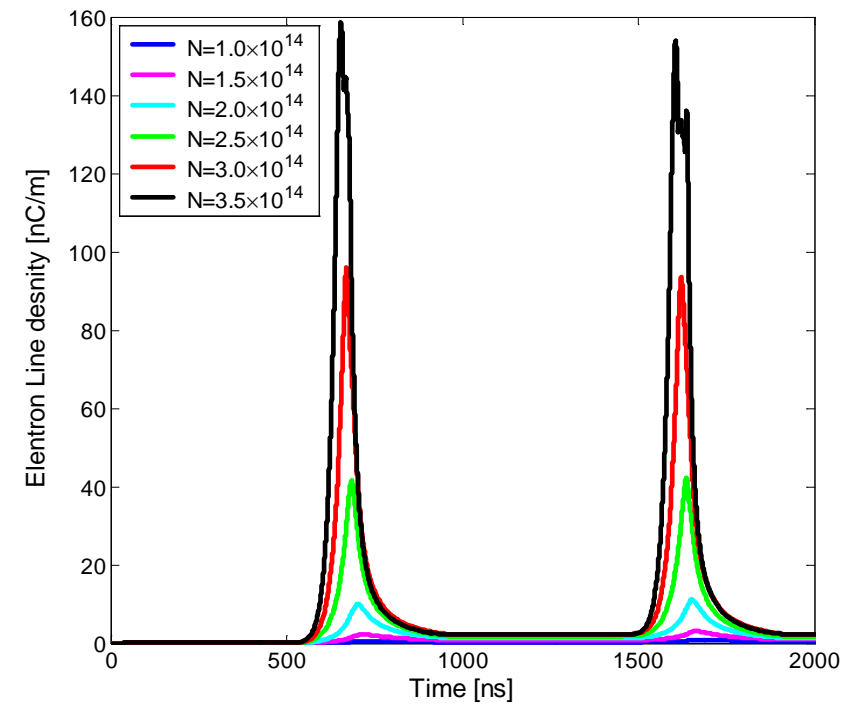
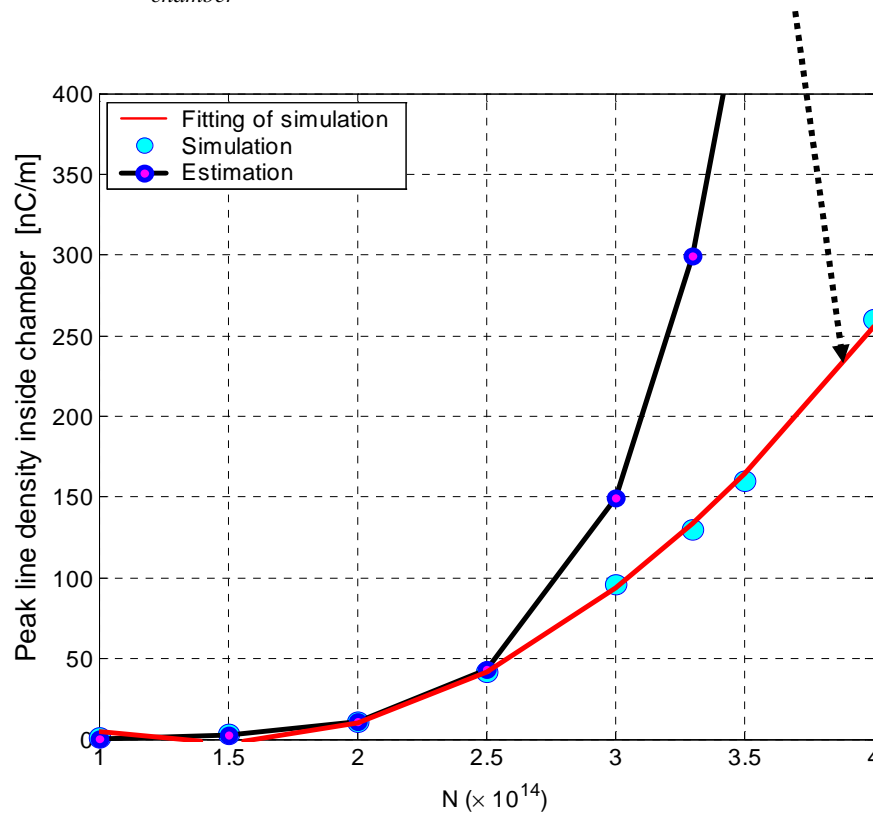
A. Browman Two-stream-2000

Beam intensity effects (I)



- High beam intensity causes high electron energy gain
- High beam intensity increases multipacting frequency $\Delta E \propto \sqrt{\lambda}$ $f_{multipacting} \propto \sqrt{\lambda}$
- Space charge slows the growth of electron density inside chamber when strong multipacting case happens

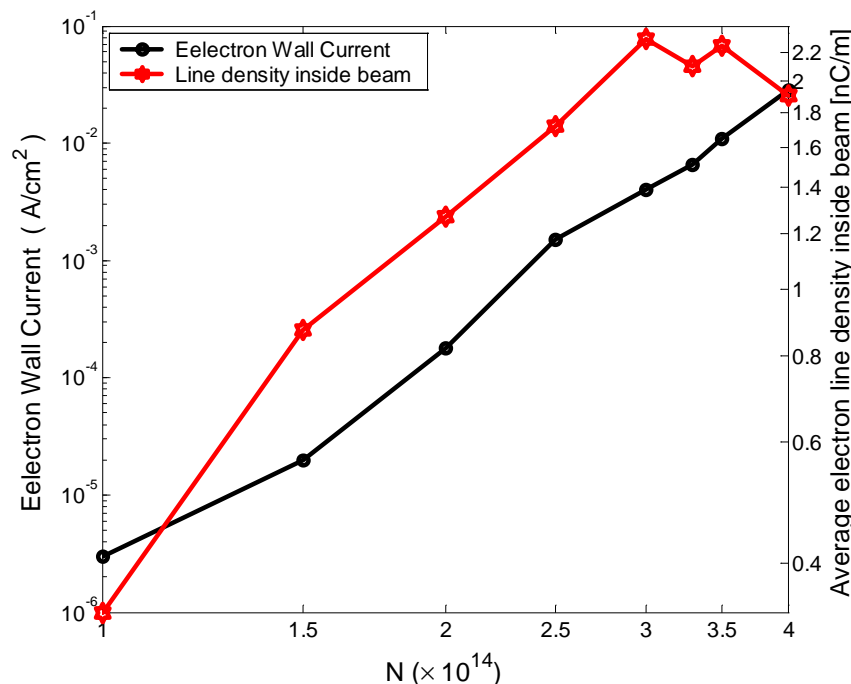
$$\lambda_{chamber} [nC/m] = 78 - 112 \times 10^{-14} N + 39 \times 10^{-28} N^2$$



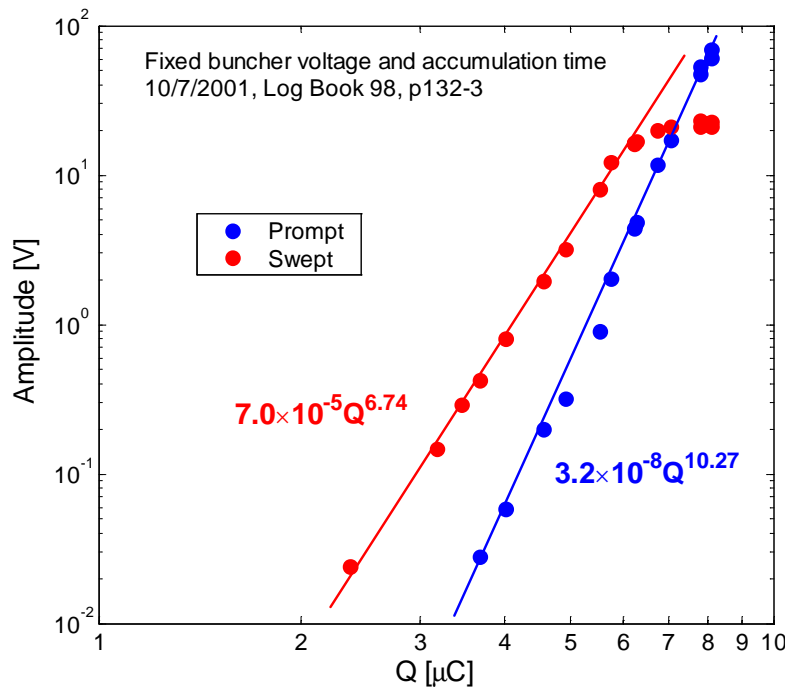
Beam intensity effects (II)



- Space charge makes the electron density inside beam saturated when strong multipacting case happens



SNS, simulation

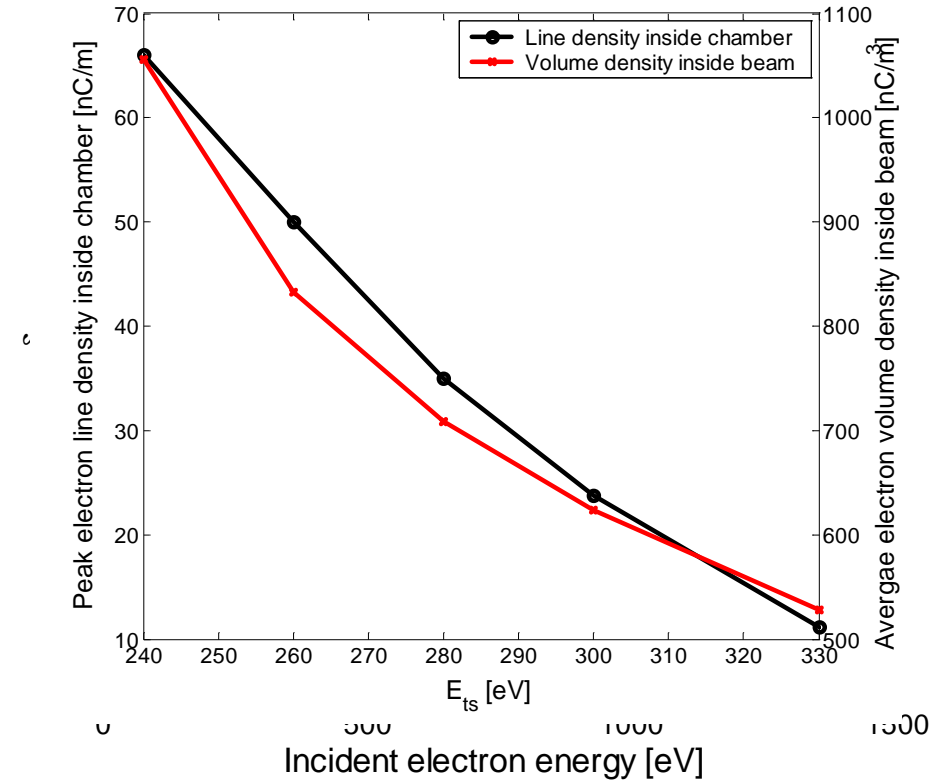
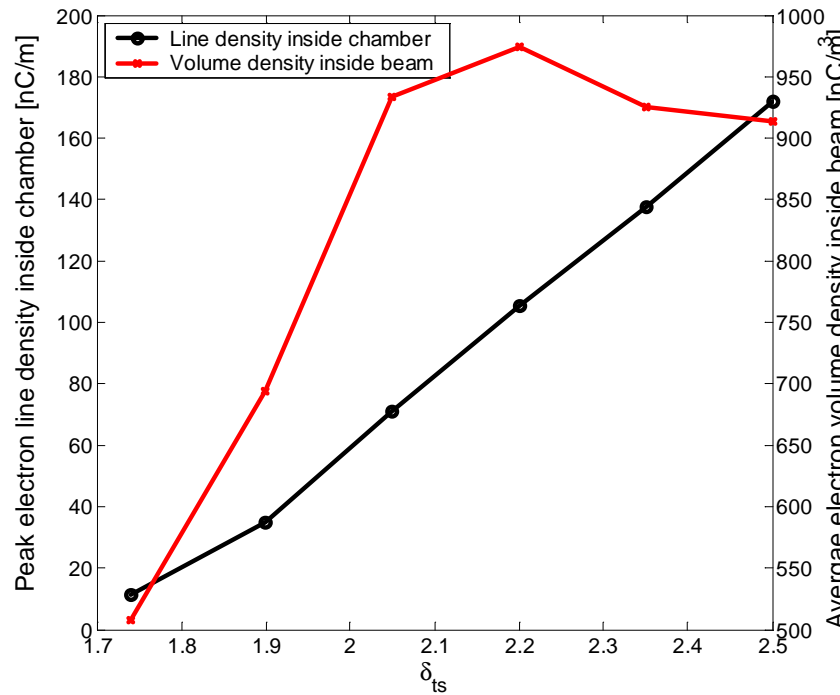


LANL PSR, Experiment, R. Macek

Peak SEY and Energy at Peak SEY



- E-cloud density inside chamber is a linear function of peak SEY and energy at peak SEY.
- E-cloud density inside chamber (and hence Instability growth rate) increases linear with peak SEY and finally saturates at some level.
- E-cloud density inside chamber (and hence Instability growth rate) decreases with the energy at peak SEY.



Electron motion in dipole magnets



- Dipole magnetic field $\mathbf{B}=(0, B_y, 0)$
- Beam electric field $\mathbf{E}=(E_x, E_y, 0)$

$$\frac{dv_y}{dt} = eE_y / m$$

$$v_x = v_{x0} \cos \omega t + v_{z0} \sin \omega t + \frac{E_{x0}}{B} \sin \omega t + \frac{1}{\omega B} \frac{dE_x}{dt} - \frac{1}{\omega B} \left(\frac{dE_x}{dt} \right)_0 \cos \omega t - \frac{1}{\omega B} \cos \omega t \int_0^t \frac{d^2 E_x}{dt^2} \cos \omega t dt - \frac{1}{\omega B} \sin \omega t \int_0^t \frac{d^2 E_x}{dt^2} \sin \omega t dt$$

$$v_z = v_{z0} \cos \omega t - v_{x0} \sin \omega t + \frac{E_{x0}}{B} \cos \omega t - \frac{E_x}{B} - \frac{1}{B} \cos \omega t \int_0^t \frac{dE_x}{dt} \cos \omega t dt + \frac{1}{B} \sin \omega t \int_0^t \frac{dE_x}{dt} \sin \omega t dt$$

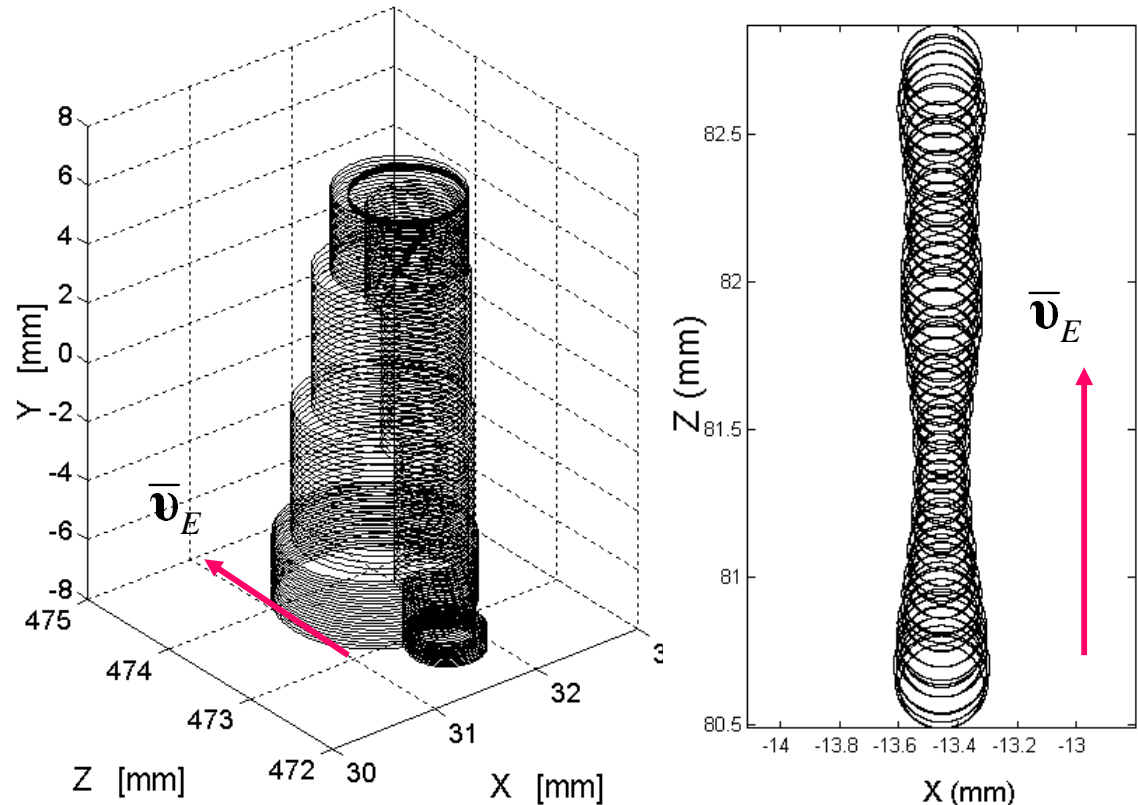
- In strong dipole magnet ($B \sim 1T$ for SNS) $\left| \frac{1}{\omega E_x} \frac{dE_x}{dt} \right| \ll 1$
- Electron motion \approx **gyration motion** + **translation** (cross-field drifting) + movement along B-field lines
- The kinetic energy of gyration motion and cross-field drifting is **smaller** comparing with the kinetic energy in B-field direction.

Electron Orbit in Dipole Magnets (Short bunch case)



Typical motion of electron in a strong dipole

- Gyration motion round B field line
- Interaction between e- and positron bunch (Receive energy from positron beam)
- $E \times B$ drift in beam direction



$$\bar{v}_E = \frac{e\mathbf{E} \times \mathbf{B}}{eB^2} = \frac{E}{B} \hat{e} \times \hat{B}$$

$$B_y = 0.1 \text{ T}$$

$$B_y = 0.8484 \text{ T}$$

Electron energy gain in strong dipole magnet

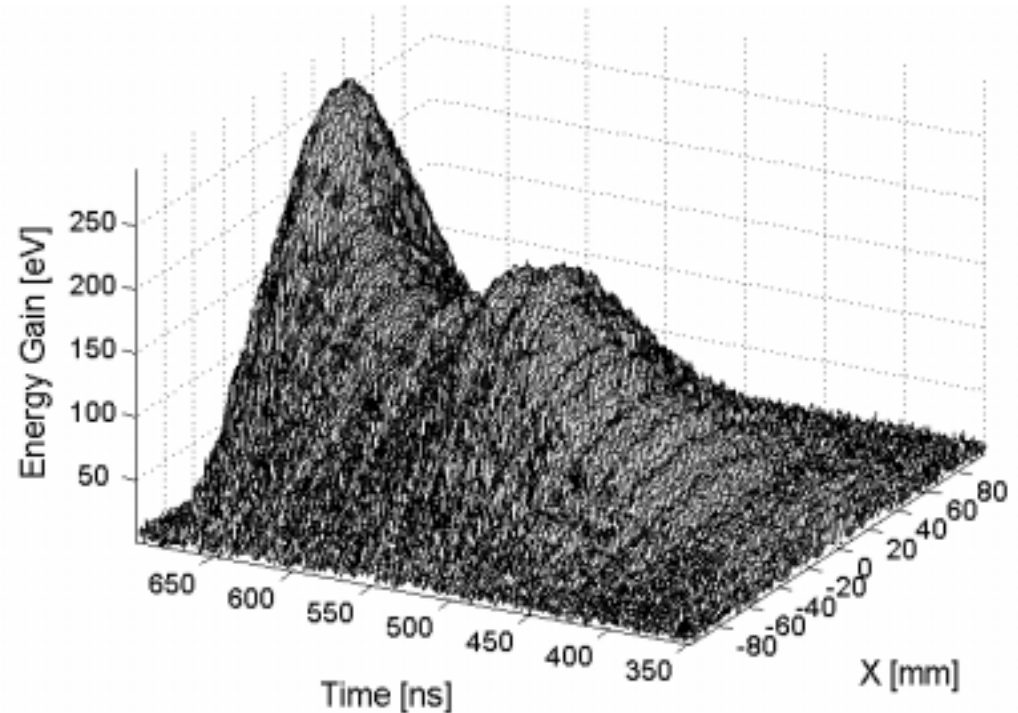
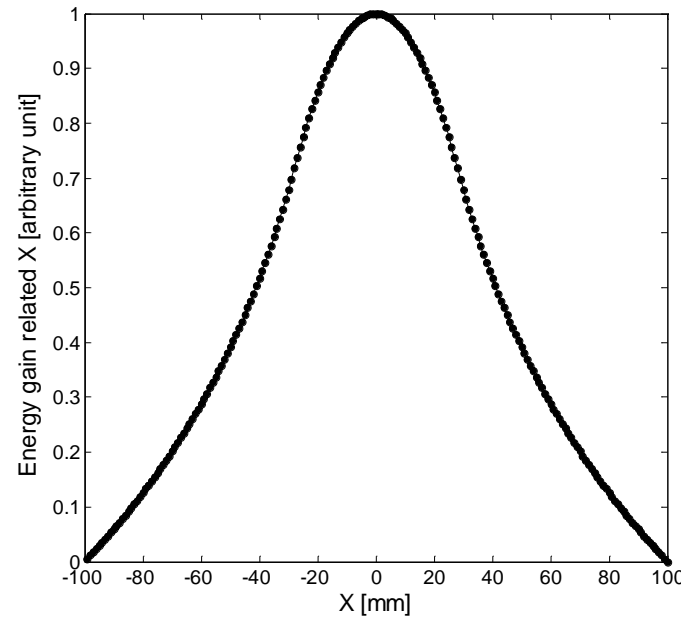


$$\Delta E(X) = -c\beta \sqrt{\frac{me}{2\pi\epsilon_0}} \frac{\partial \lambda}{\partial z} \frac{1}{\sqrt{\lambda}} \left(1 - \frac{X^2}{a^2} + \ln \frac{b^2}{a^2} \right) \left(aG + \int_{\sqrt{a^2-X^2}}^{\sqrt{b^2-X^2}} \left(\ln \frac{b^2}{X^2+y^2} \right)^{-1/2} dy \right) \\ + \frac{1}{2} c\beta \sqrt{\frac{me}{2\pi\epsilon_0}} \frac{\partial \lambda}{\partial z} \frac{1}{\sqrt{\lambda}} \int_0^{\sqrt{a^2-X^2}} \frac{y^2}{a^2} \left[\ln \left(1 - \frac{X^2}{a^2} + \ln \frac{b^2}{a^2} + \frac{y^2}{a^2} \right) \right]^{-1/2} dy \\ + \frac{1}{2} c\beta \sqrt{\frac{me}{2\pi\epsilon_0}} \frac{\partial \lambda}{\partial z} \frac{1}{\sqrt{\lambda}} \int_{\sqrt{a^2-X^2}}^{\sqrt{b^2-X^2}} \left(1 - \frac{X^2}{a^2} + \ln \frac{X^2+y^2}{a^2} \right) \left[\ln \left(\frac{b^2}{X^2+y^2} \right) \right]^{-1/2} dy \quad (|X| < a)$$

$$\Delta E(X) = -c\beta \sqrt{\frac{me}{2\pi\epsilon_0}} \frac{\partial \lambda}{\partial z} \frac{1}{\sqrt{\lambda}} \left[\frac{b^2}{X^2} \int_0^{\sqrt{b^2-X^2}} \left(\ln \frac{b^2}{X^2+y^2} \right)^{-1/2} dy - \frac{1}{2} \int_0^{\sqrt{b^2-X^2}} \frac{X^2+y^2}{X^2} \left(\ln \frac{b^2}{X^2+y^2} \right)^{-1/2} dy \right]$$

$$G = \arcsin \left[\frac{\sqrt{a^2 - X^2}}{a} \left(1 - \frac{X^2}{a^2} + \ln \frac{b^2}{X^2+a^2} \right)^{-1/2} \right] \quad (|X| > a)$$

Electron energy gain in strong dipole magnet

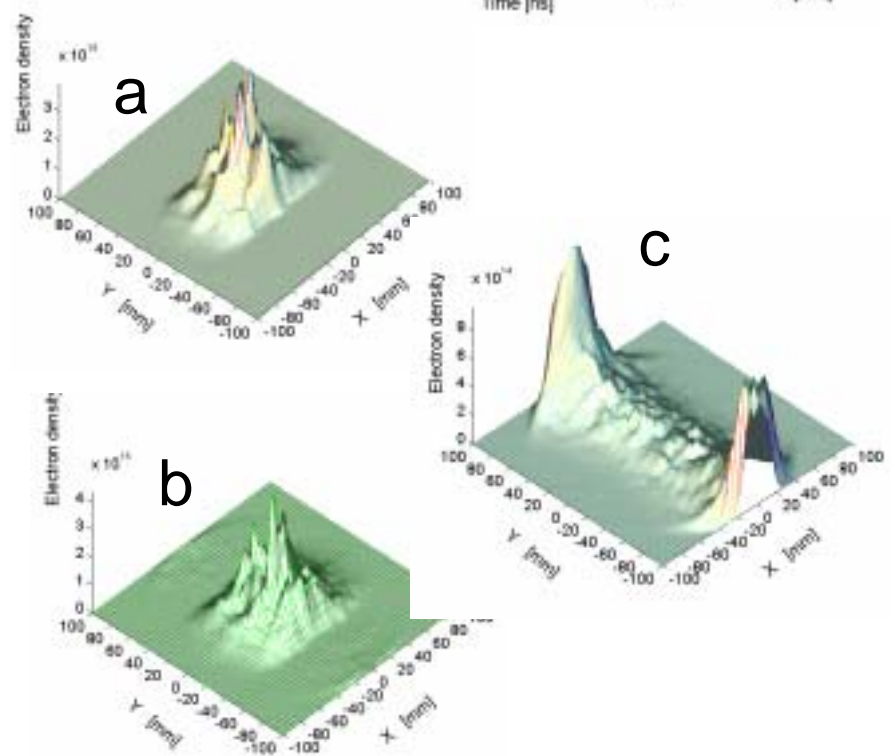
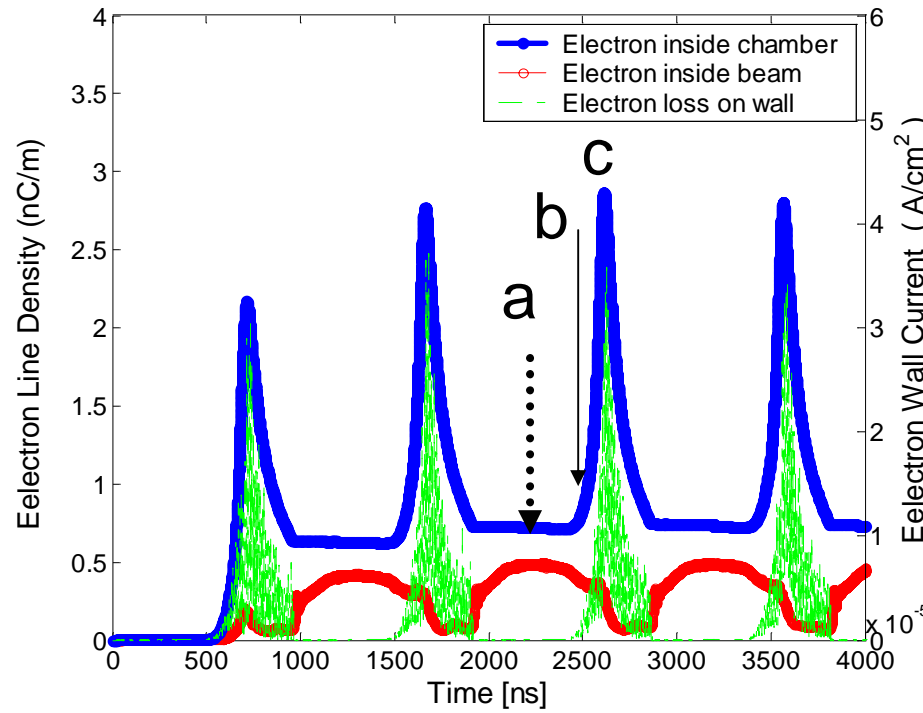


Energy gain at the wall surface for different X-coordinates. Left plot shows the electron energy gain as a function of horizontal coordinate. It is normalized by the peak energy gain at the chamber center $X=0$. Right plot shows the energy gain of direct drifting electrons in SNS dipole magnets with $B_y=7935$ Gauss.

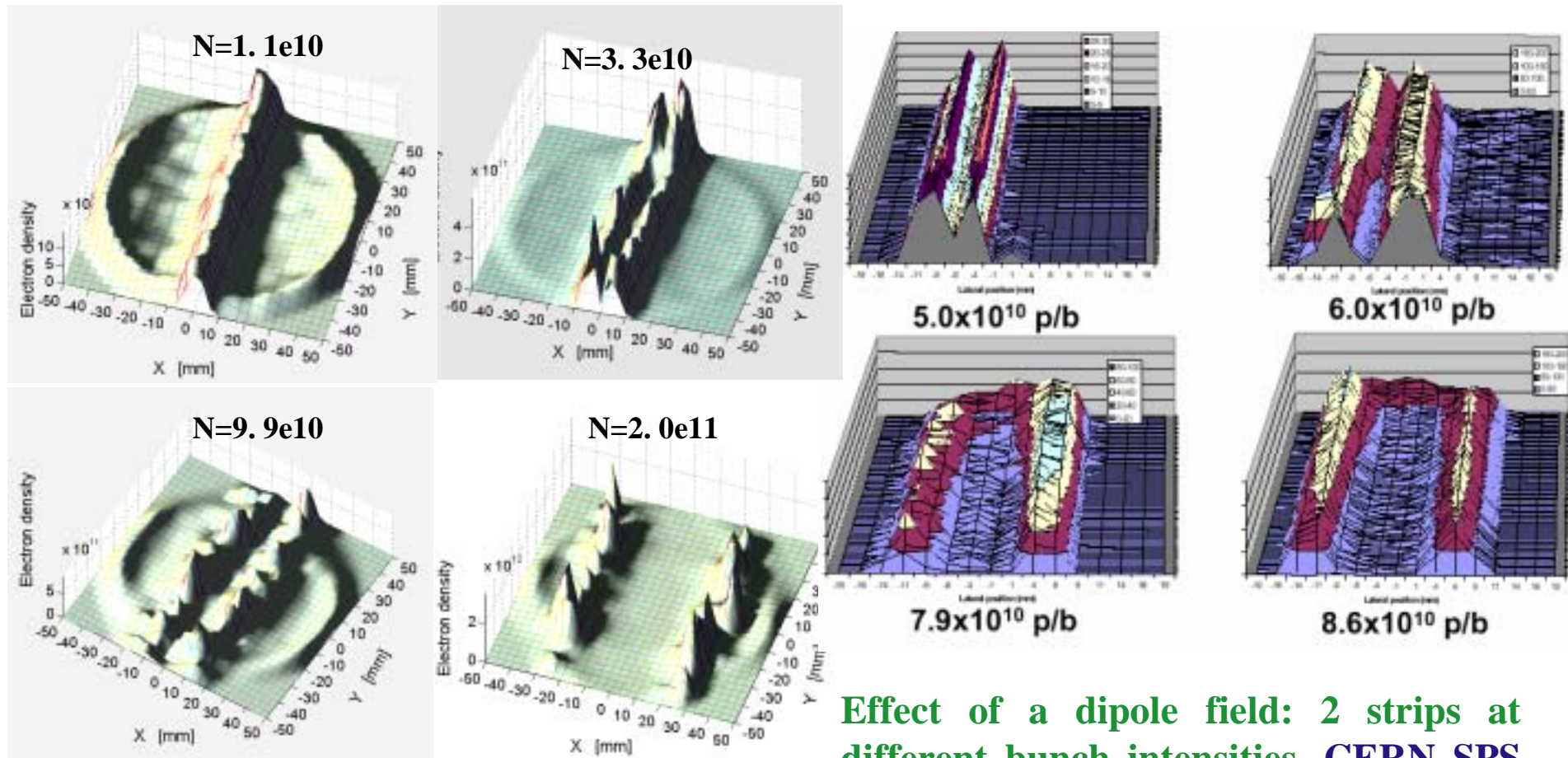
Multipacting in Dipole magnets (By=0.79T)



- Multipacting happen at the horizontal chamber center (**1 strip**, agree with estimation)
- E-cloud density is **about 2 times smaller** than the drift region



Bunch current effects on Multipacting in *dipole* for *short bunch--strip position* and lost charge density



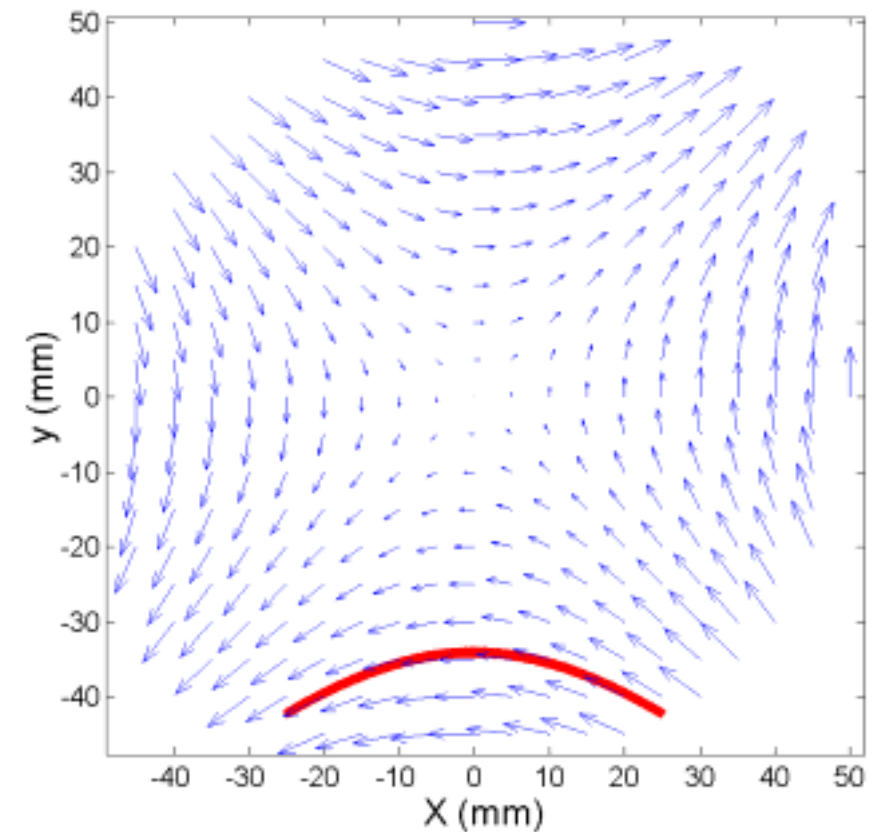
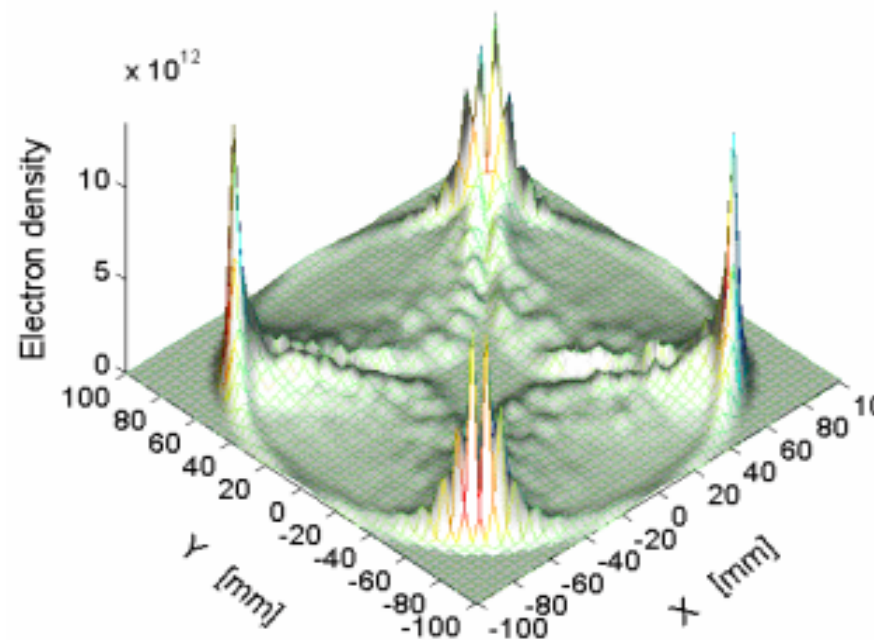
KEKB LER, simulation

Effect of a dipole field: 2 strips at different bunch intensities, CERN SPS experimental results, J. M.Jimenez, ECloud'02, CERN, 2002

E-cloud in Quadrupole and Sextupole magnets



Ecloud in quadrupole



- Weak multipacting happens only near the middle of the pole surface
- No Trapping for long bunch! (trap was suspected in PSR, PSR-94-005)

Trapping mechanism II --- Beam potential effect

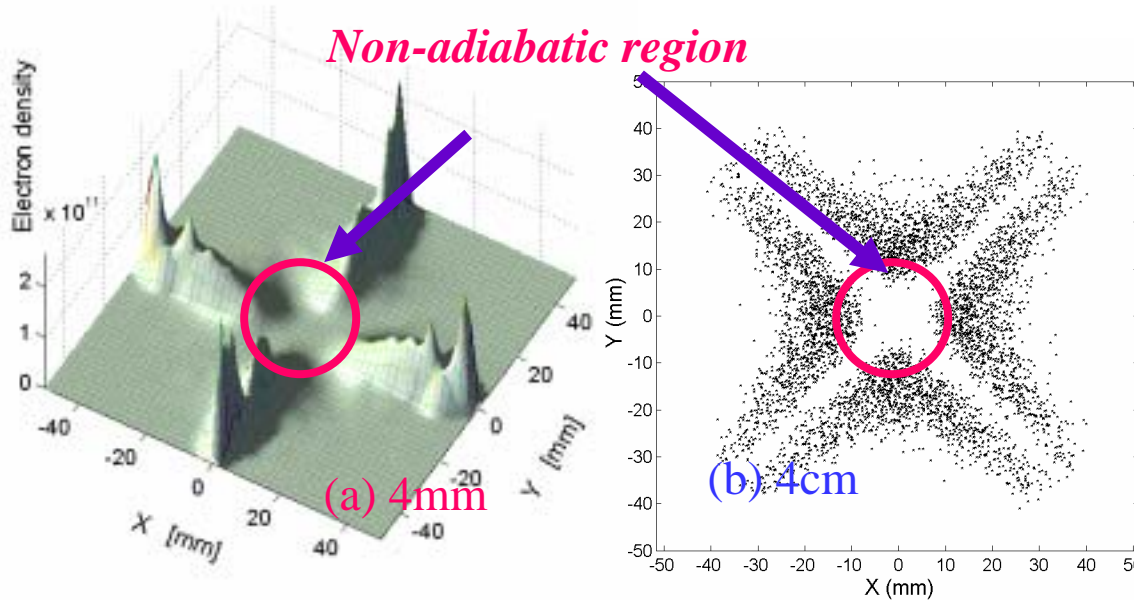
(PRE 66, 036502, 2002)



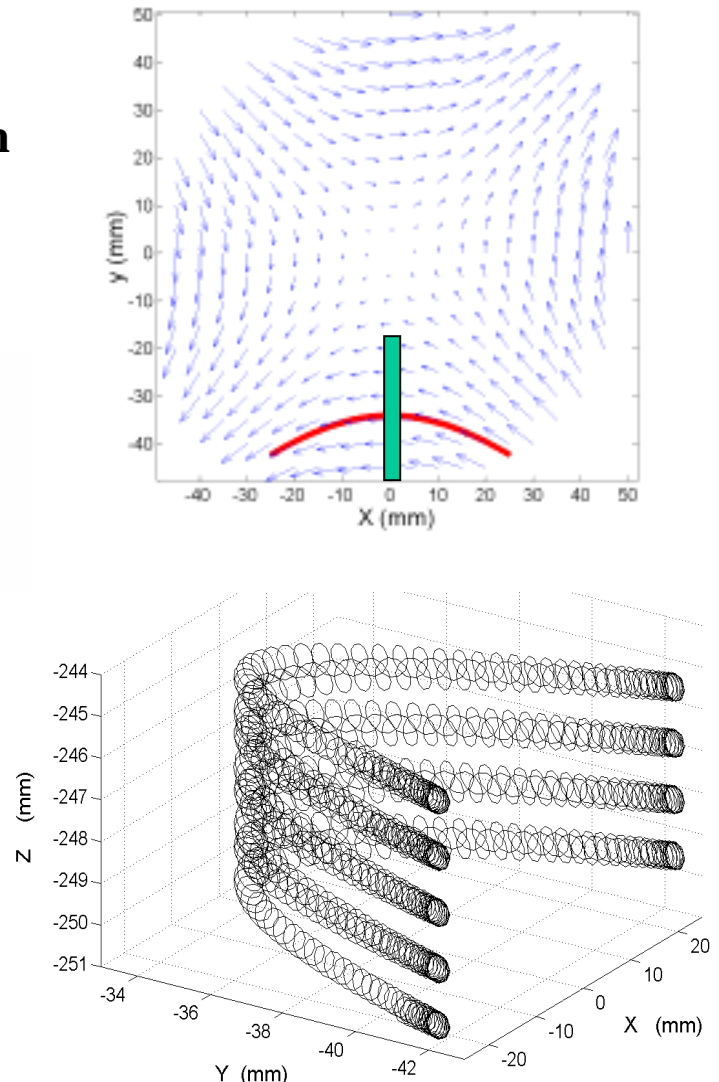
Trap requirement for positron bunch

Bunch length should be shorter than period of gyration

motion $\sigma_l < \frac{2\pi cm}{e} \frac{1}{B} \rightarrow \sigma_l (mm) < 10.7 / B(T)$



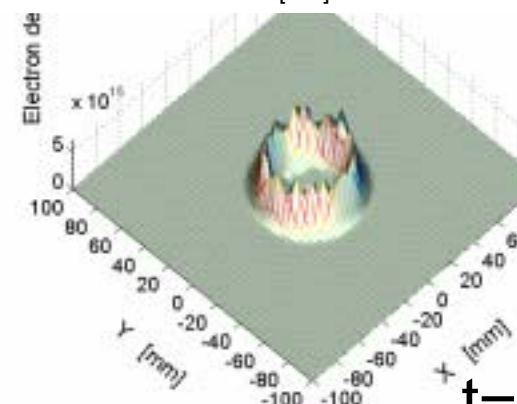
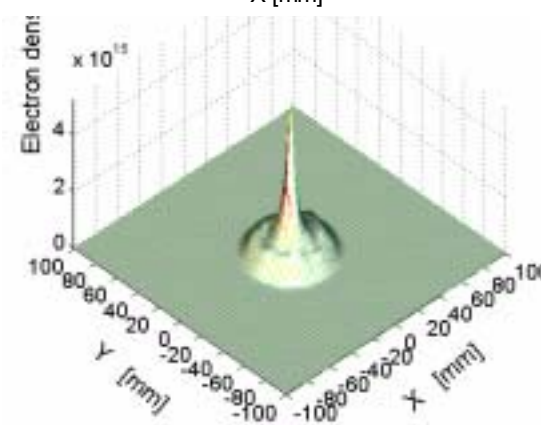
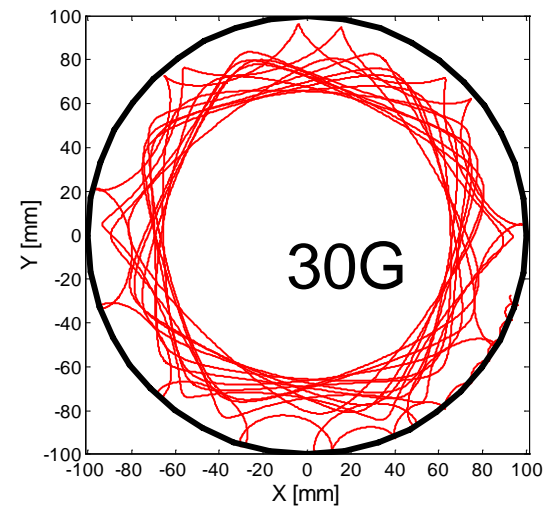
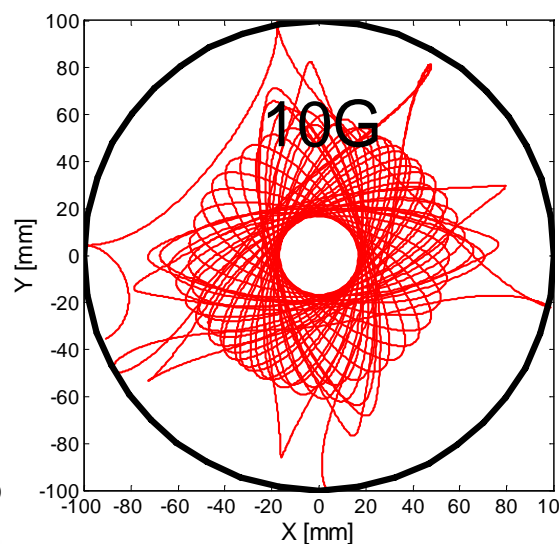
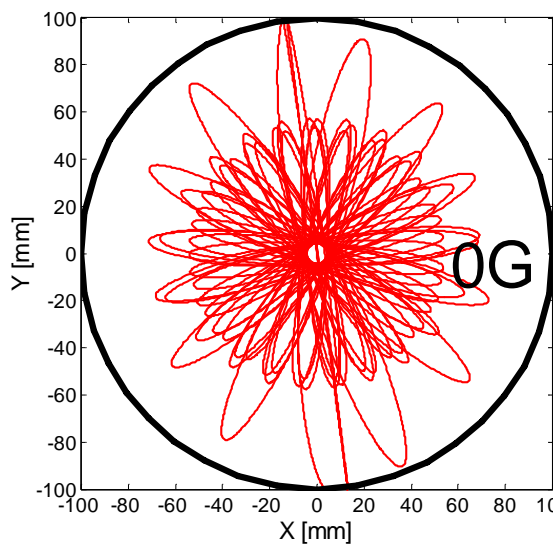
Trapped photoelectron distribution in quadrupole magnet with field gradient 10.3 T/m during the train gap for different bunch length



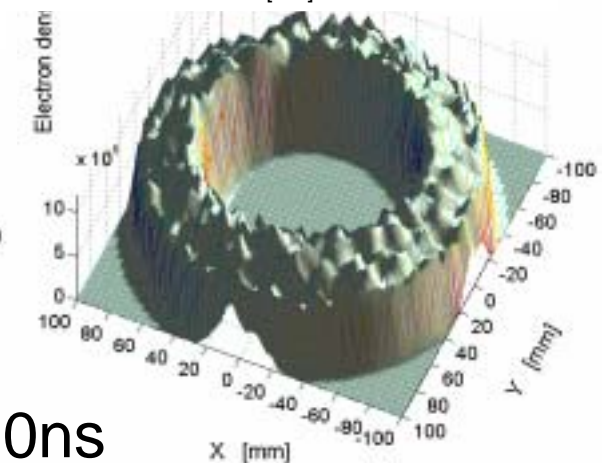
Uniform Solenoid effects



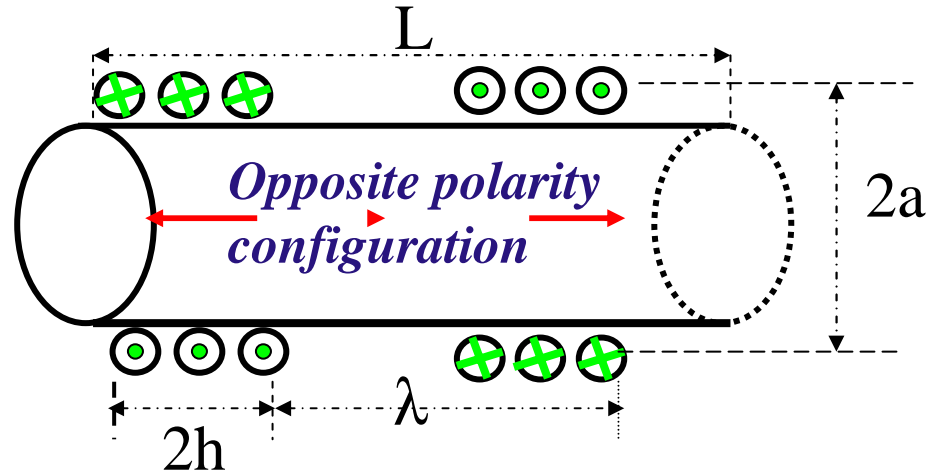
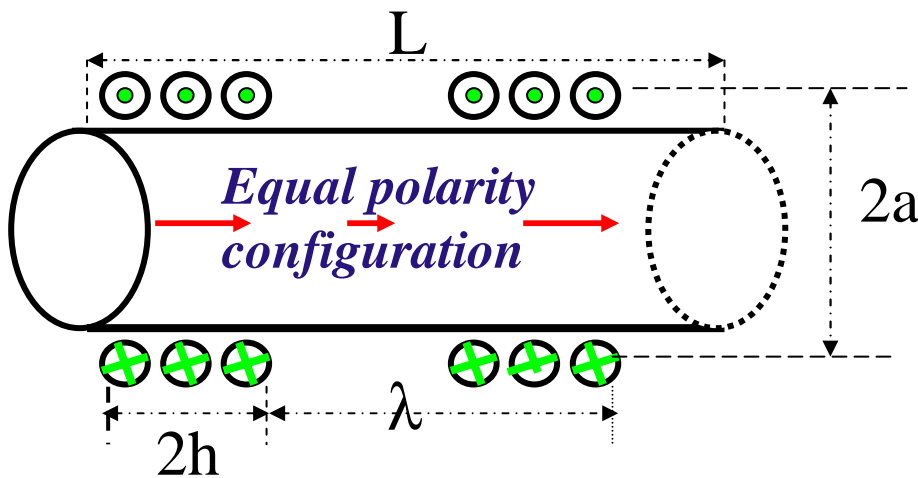
- 30G Solenoid field can reduce the e-cloud density with a factor 2000 !
- Zero density within beam



$t=350\text{ns}$



Solenoid---Configuration



$$B_r = B_0 \frac{2ka}{\pi} \sum_{n=1}^{\infty} \sin nhk K_1(nka) I_1(nkr) \sin nkz$$

$$B_z = B_0 \left(\frac{2h}{\lambda} + \frac{2ka}{\pi} \sum_{n=1}^{\infty} \sin nhk K_1(nka) I_0(nkr) \cos nkz \right)$$

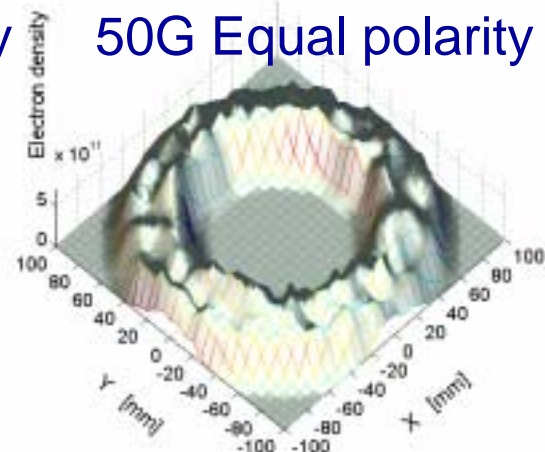
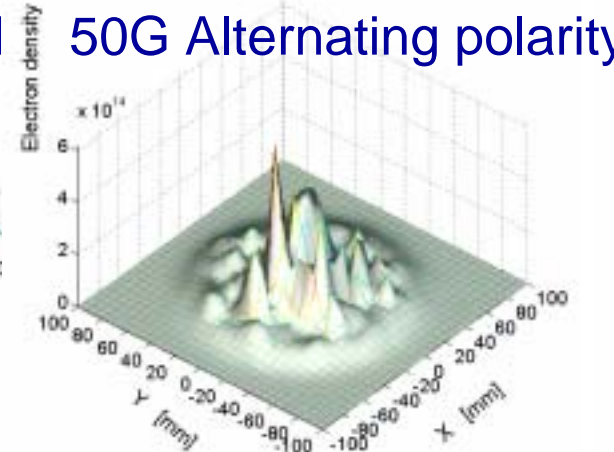
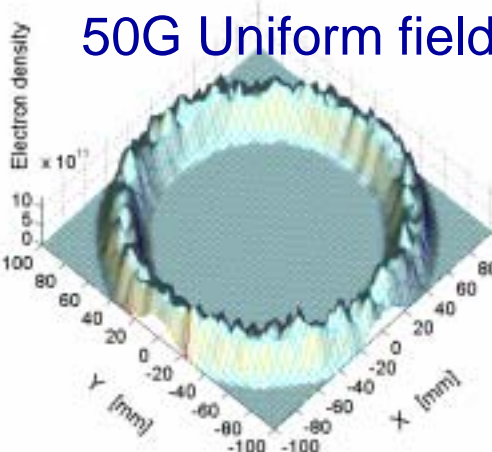
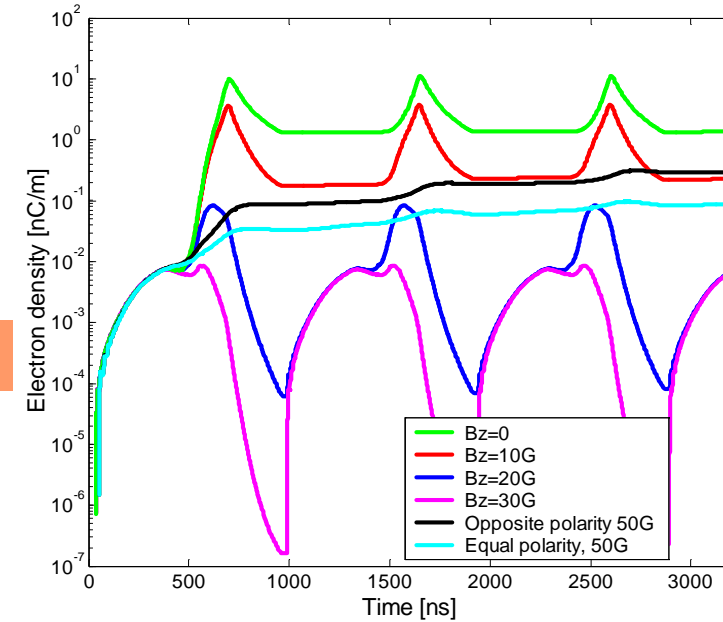
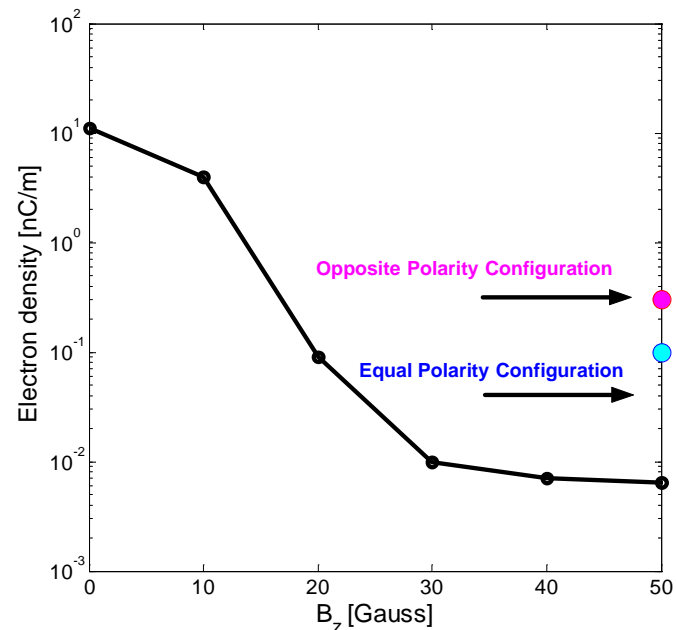
$$B_r = B_0 \frac{4ka}{\pi} \sum_{n=1,3,5}^{\infty} \sin nhk K_1(nka) I_1(nkr) \sin nkz$$

$$B_z = B_0 \frac{4ka}{\pi} \sum_{n=1,3,5}^{\infty} \sin nhk K_1(nka) I_0(nkr) \cos nkz$$

By E. Perevedentsev

$B_0 = 50$ Gauss, $h = 0.4$ m, $a = 120$ mm, $\lambda = 1$ m and 2 m

Solenoid configuration effects



50G Uniform field

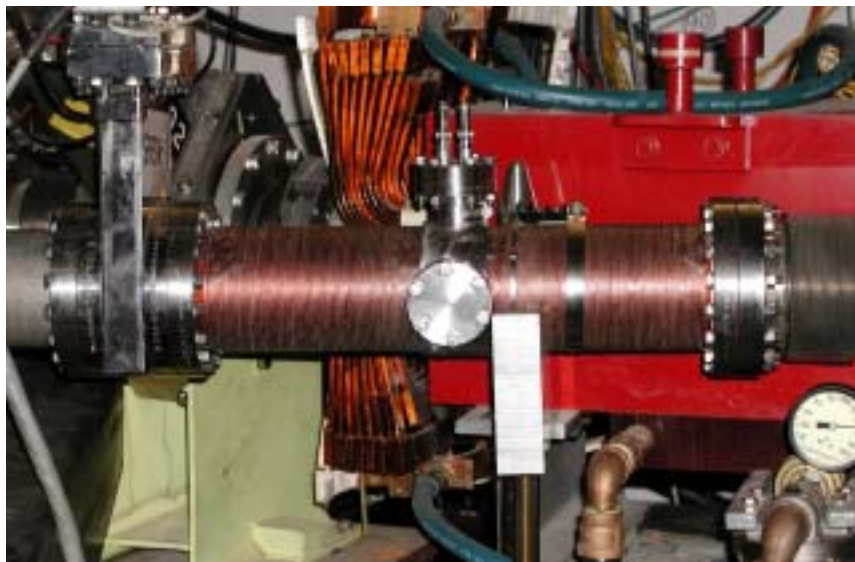
50G Alternating polarity

50G Equal polarity

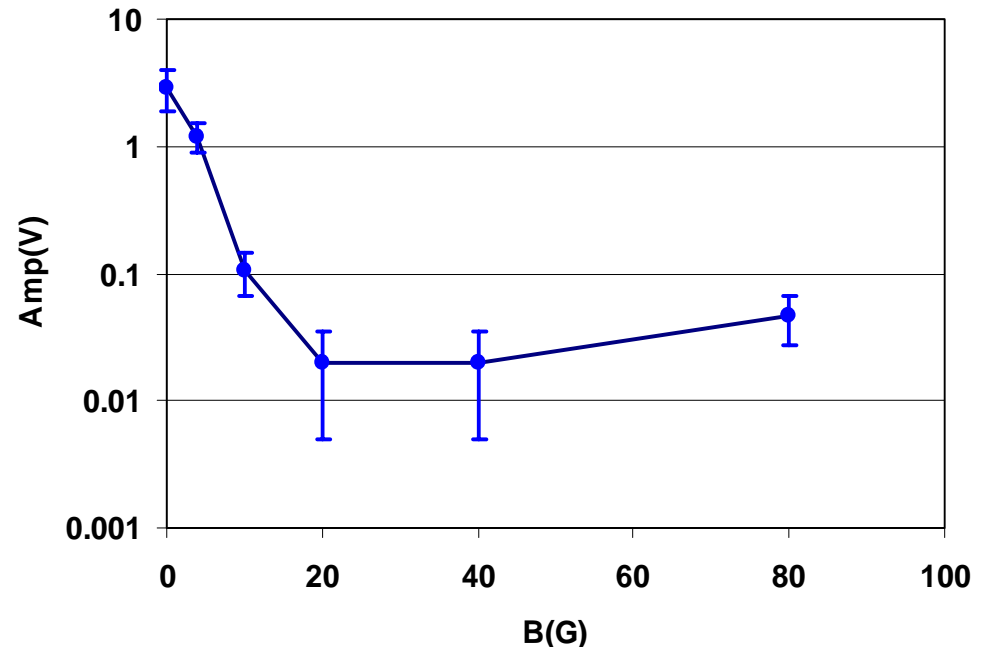
Solenoid effect on electron signal -----PSR experiment



- 20G Solenoid field can reduce the e-cloud signal with a factor > 50 !
- 10% of the ring is covered by solenoid, but solenoid has no effect no the instability thresh!

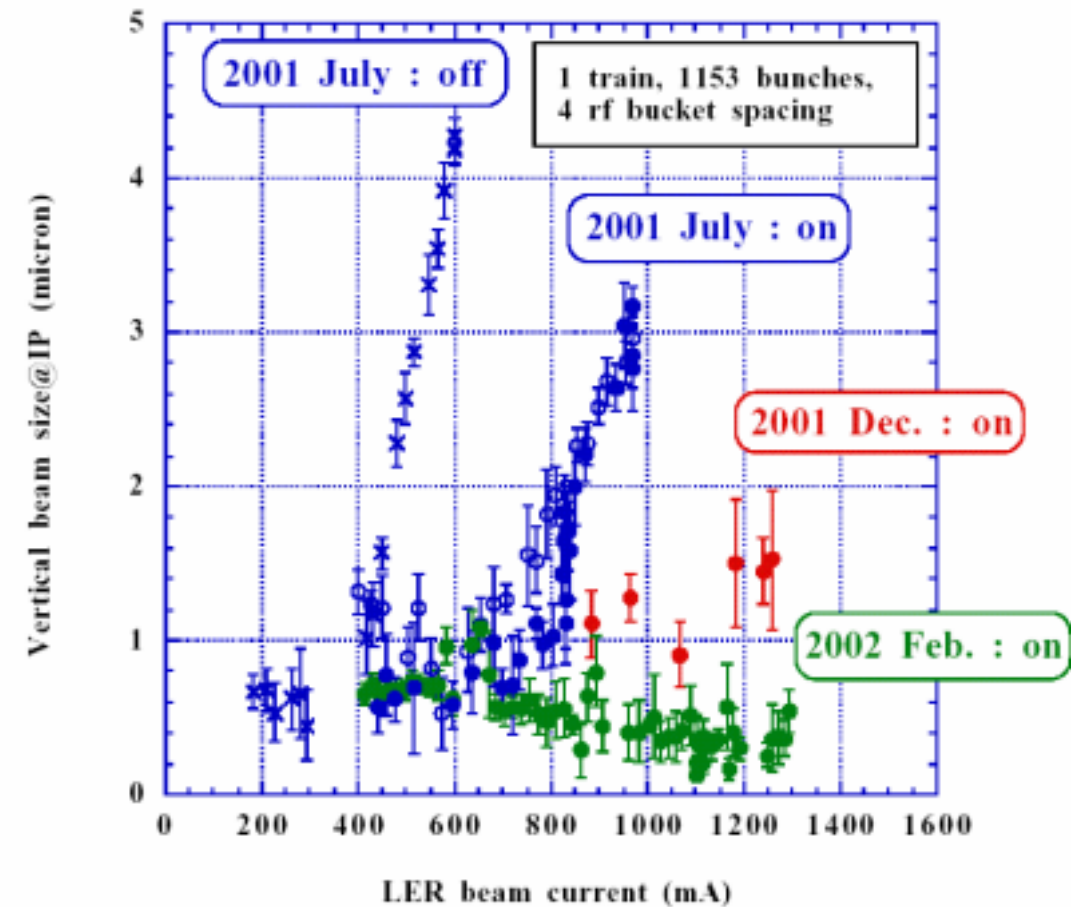


Picture of RFA (ED92Y) in a short solenoid in section 9



Effect of weak solenoid on prompt electron peak (ED92Y)

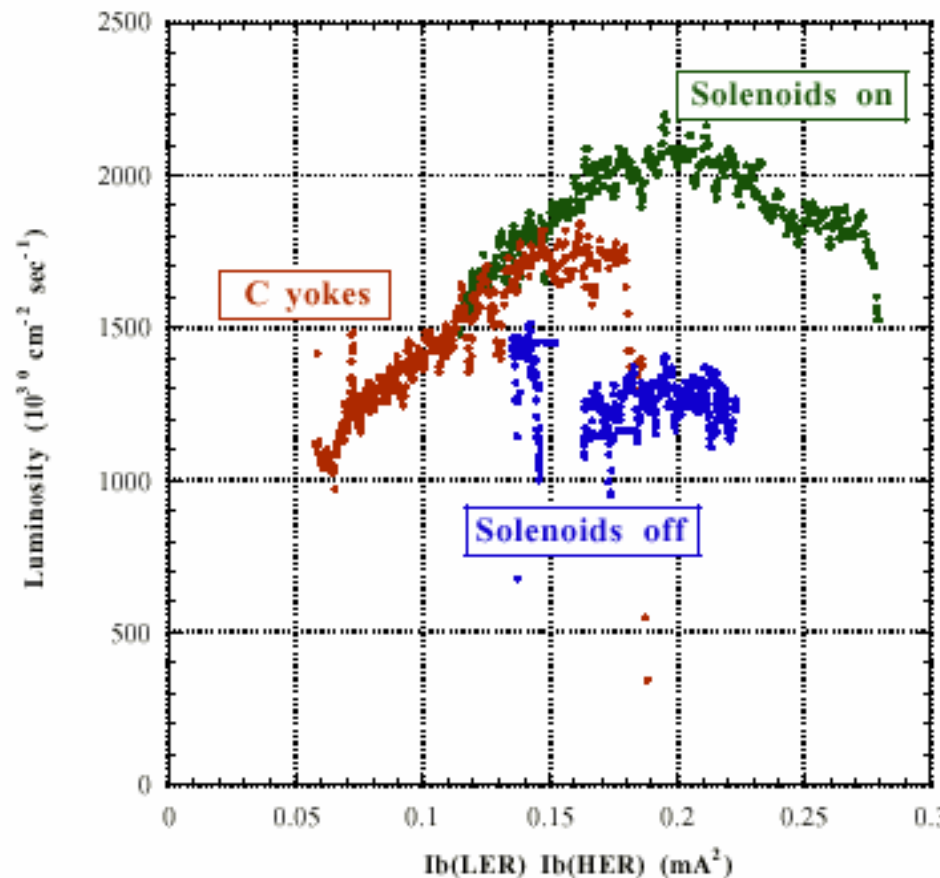
Solenoid effect on beam size in KEKB LER



H. Fukuma, e-cloud'02

After last installation of solenoid, blowup was disappeared up to 1300mA.

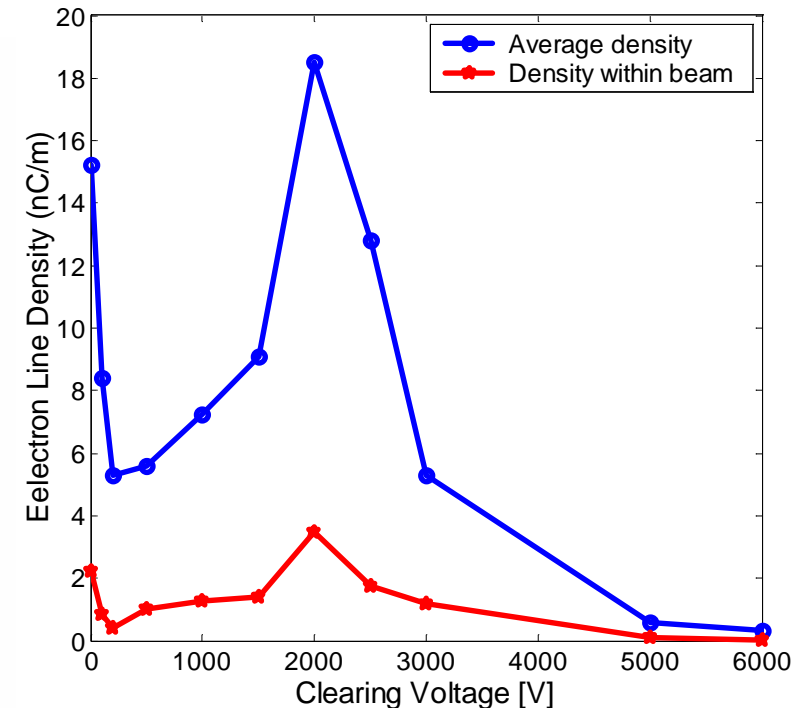
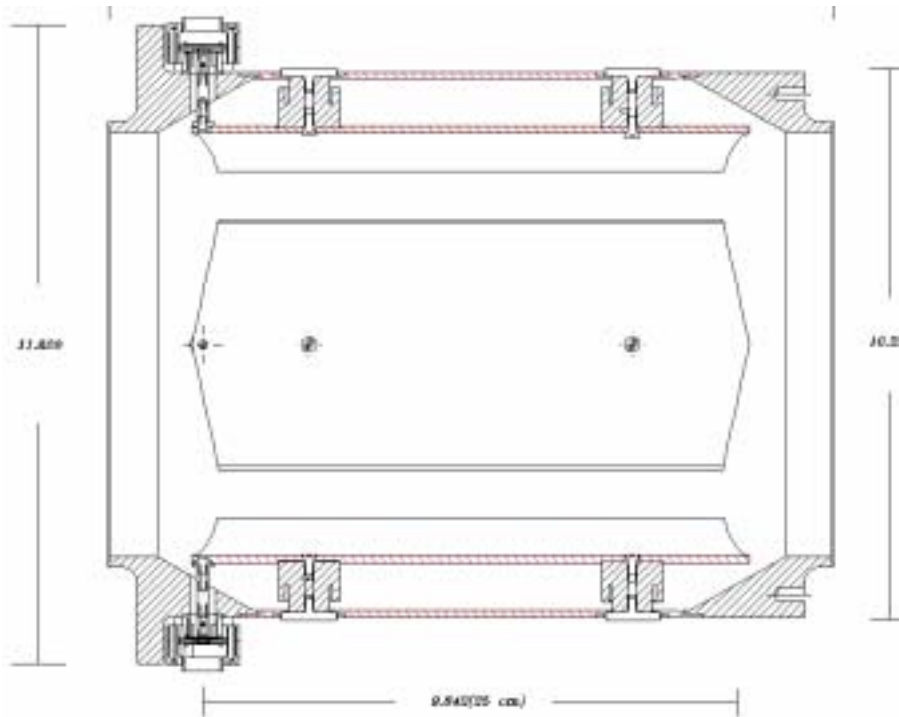
Solenoid effects on luminosity



Electrode clearing effect vs. Clearing voltage



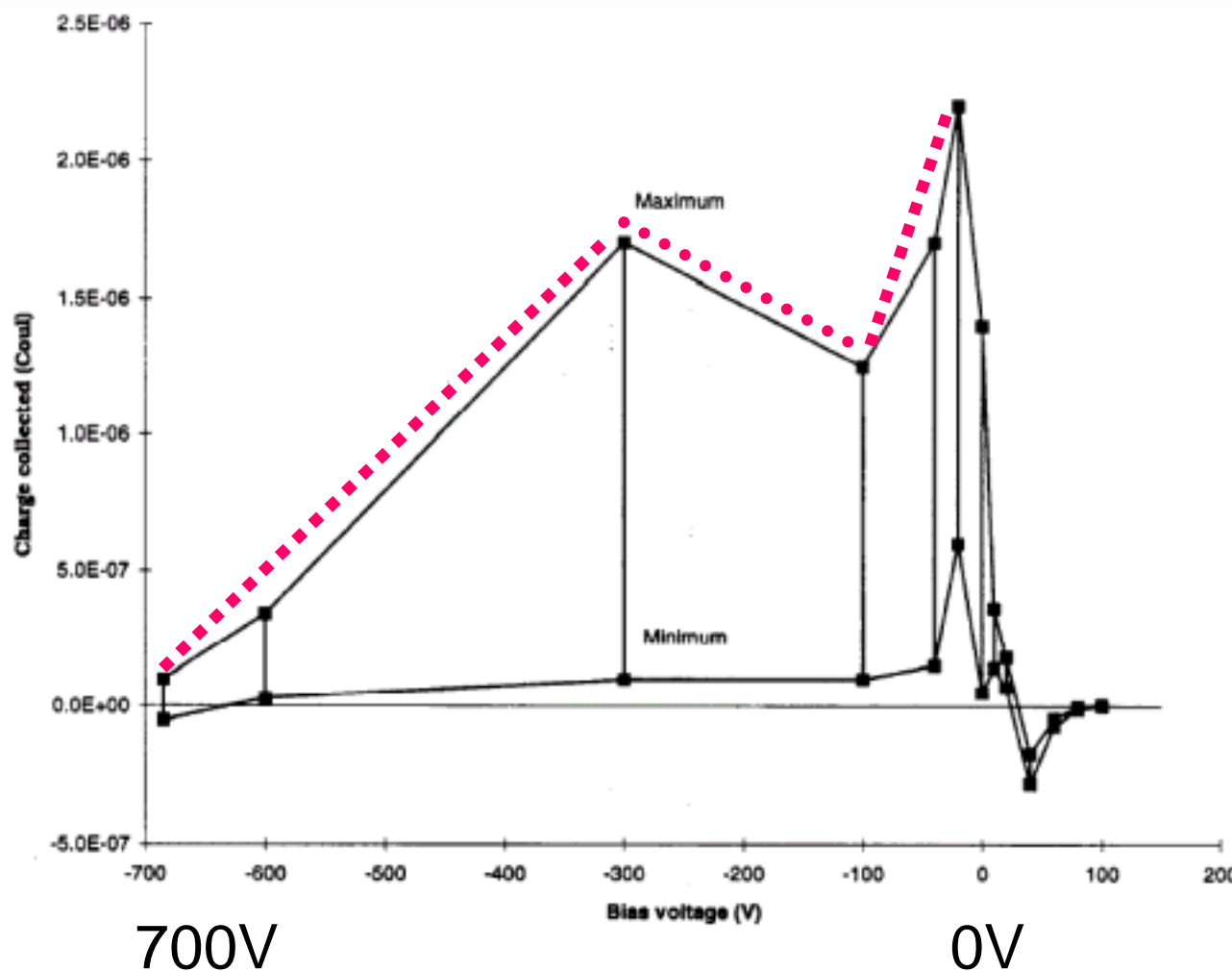
(Accepted by PRSTAB)



e-cloud density vs. clearing fields

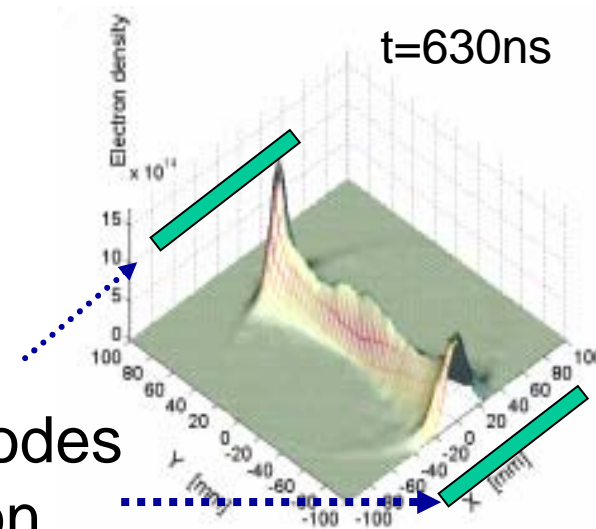
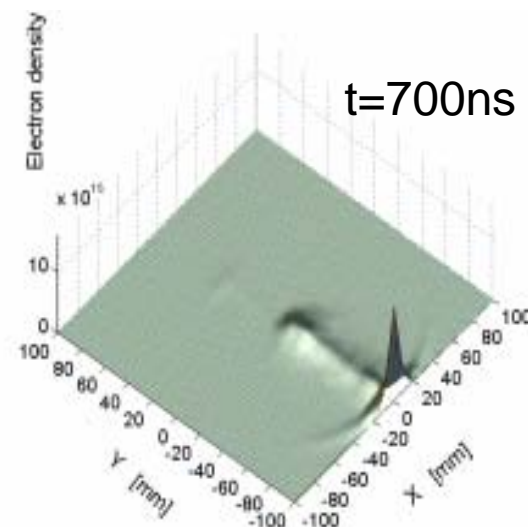
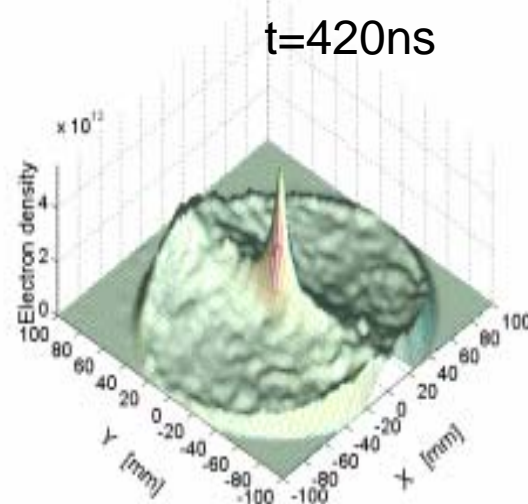
- Weak field(~200V) is very helpful
- Strong multipacting at 2kV, which could be stronger than zero field case

PSR(PSR-94-03,M. Plum, etc.)



PSR experiment

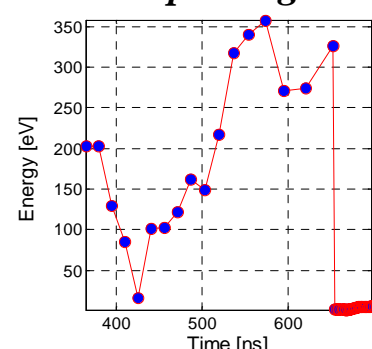
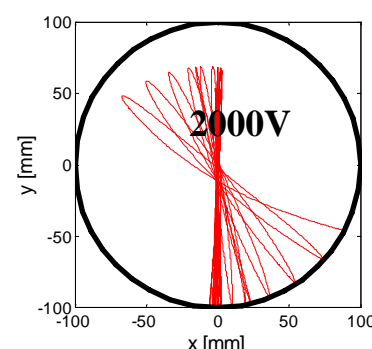
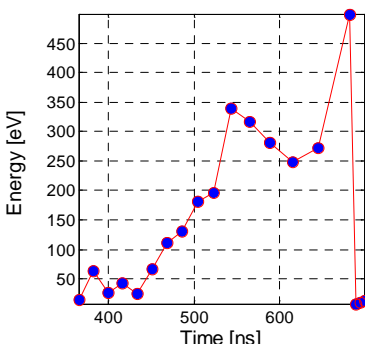
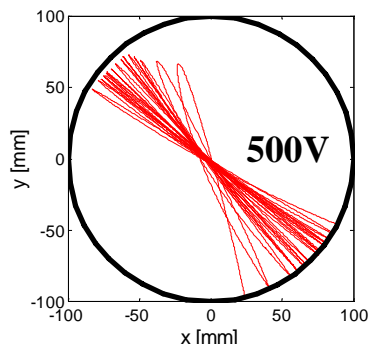
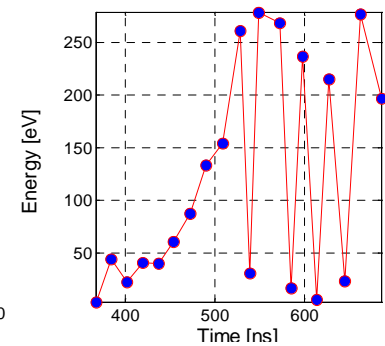
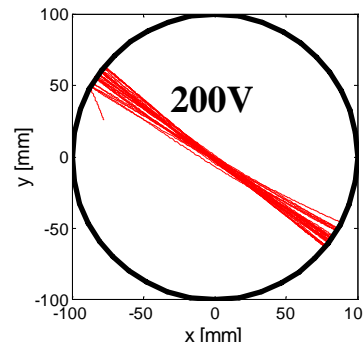
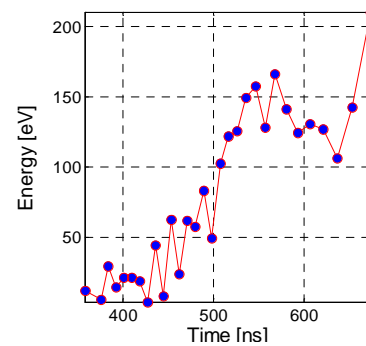
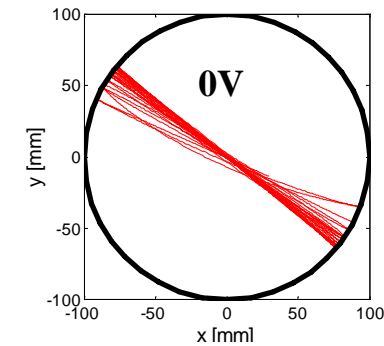
E-cloud distribution at different time for 500V clearing field



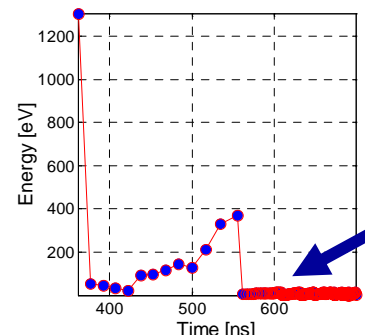
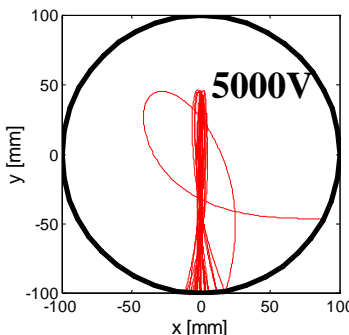
Electrodes
position

- Clearing field can cause the particle polarized toward the clearing field direction. As a result, it causes strong multipacting near the positive electrode.

Mechanism of strong multipacting due to clearing field



half multipacting frequency



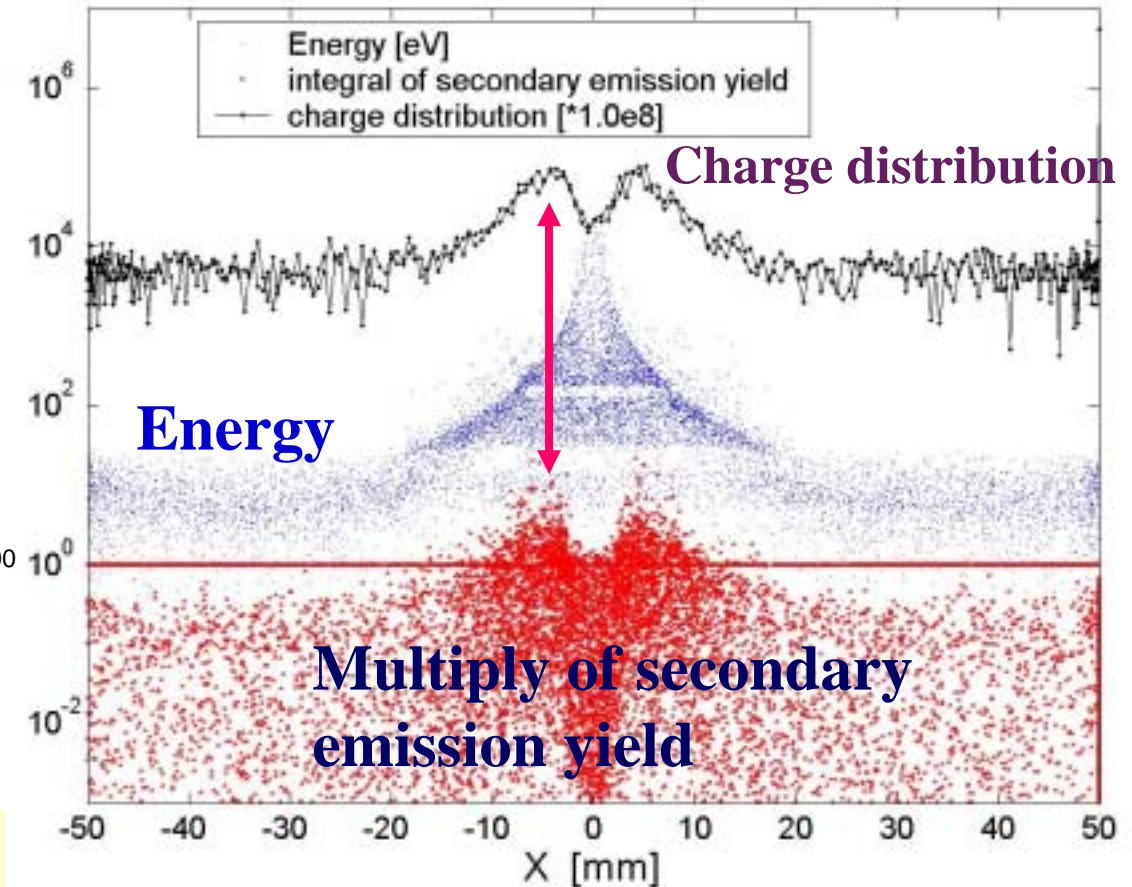
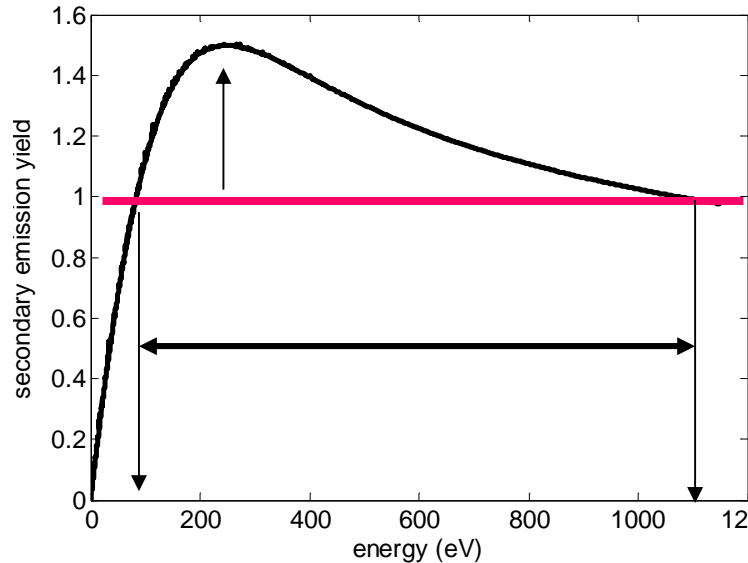
Mechanism of clearing of electron cloud is to suppress the second emission at the chamber surface at the bunch tail. $E_{\text{clearing}} > E_{\text{beam}}$

Summary



- Electron motion under beam space charge field is investigated. (Adiabatic invariant, Nonlinear oscillation frequency, electron energy gain). Mechanism of trailing edge multipacting is clearly explained
- Many factors related to the multipacting has been investigated one by one using 3D code. The results qualitatively agree with the our analysis and experiment studies. Beam intensity, Longitudinal beam profile, transverse beam size, beam in gap are important.
- Good agreement is achieved between analysis and simulation for the multipacting in drift region and dipole magnet
- Multipacting in Quad and Sextupole is very weak. There is no mirror field trapping due to the long bunch length
- Solenoid is a good remedy (convenient and effective), but clearing electrode is complicated.

Mechanism of multipacting in Dipole magnet

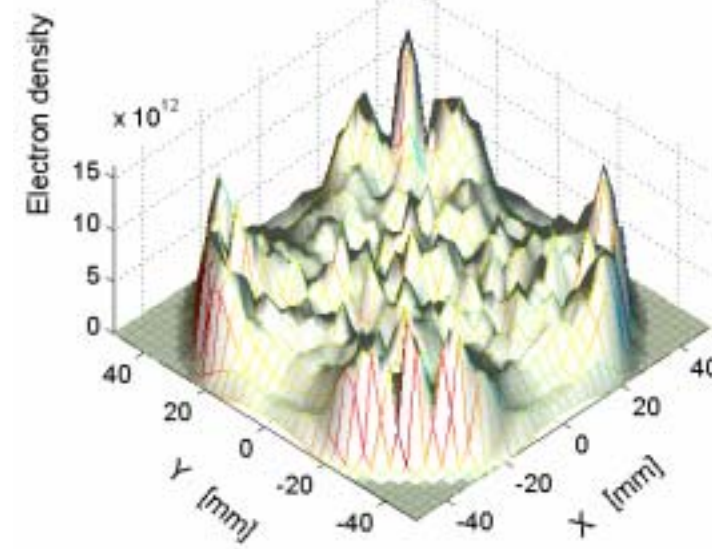
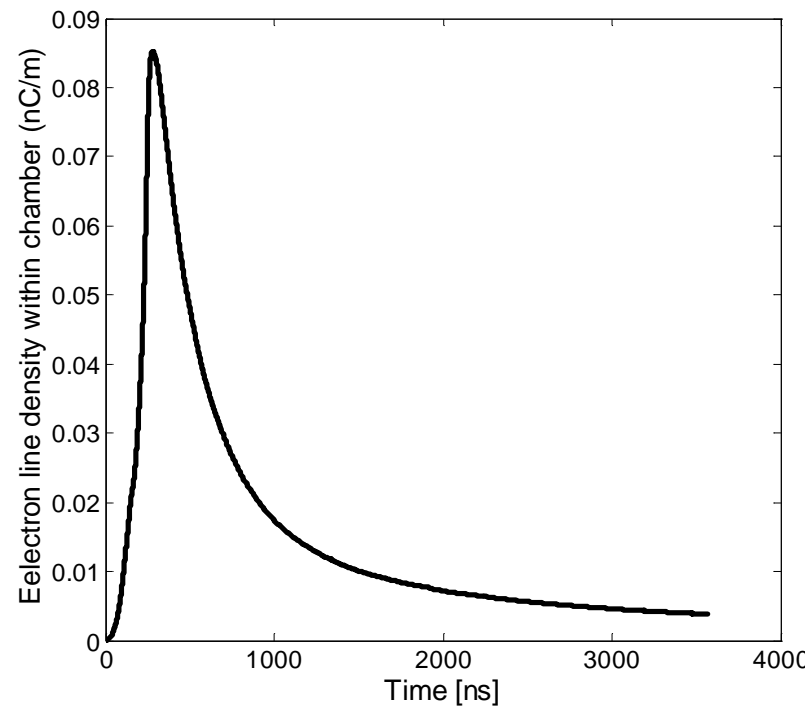


If $Y_2 > 1 \Rightarrow$ multi-pacting

If $Y_2 < 1 \Rightarrow$ no multi-pacting

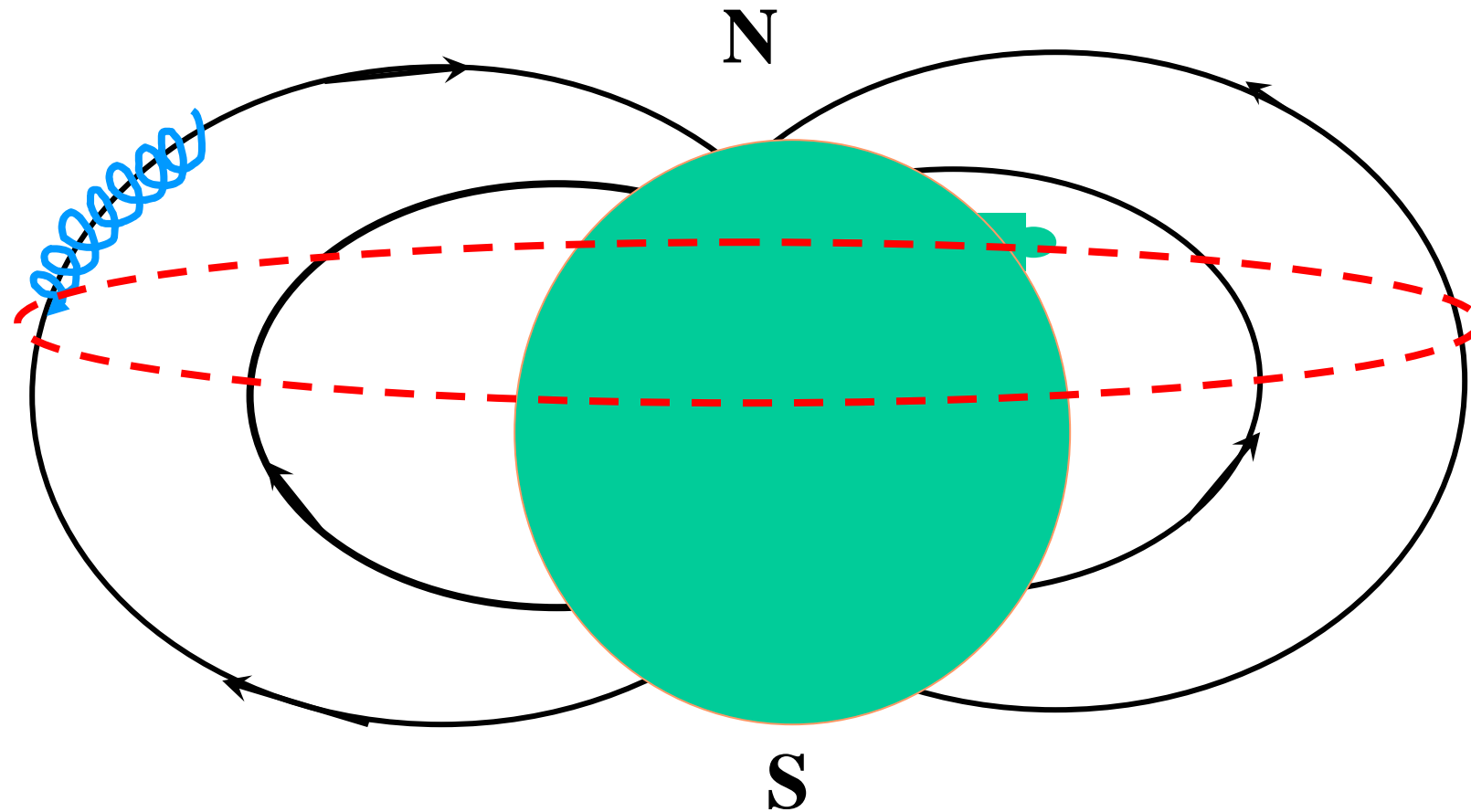
Energy, Charge and Y_2 distribution of the lost electrons

E-cloud in PSR Quadrupole



- Very weak multipacting
- Long decay time, but there is not trapping

Particle trapping in the sky

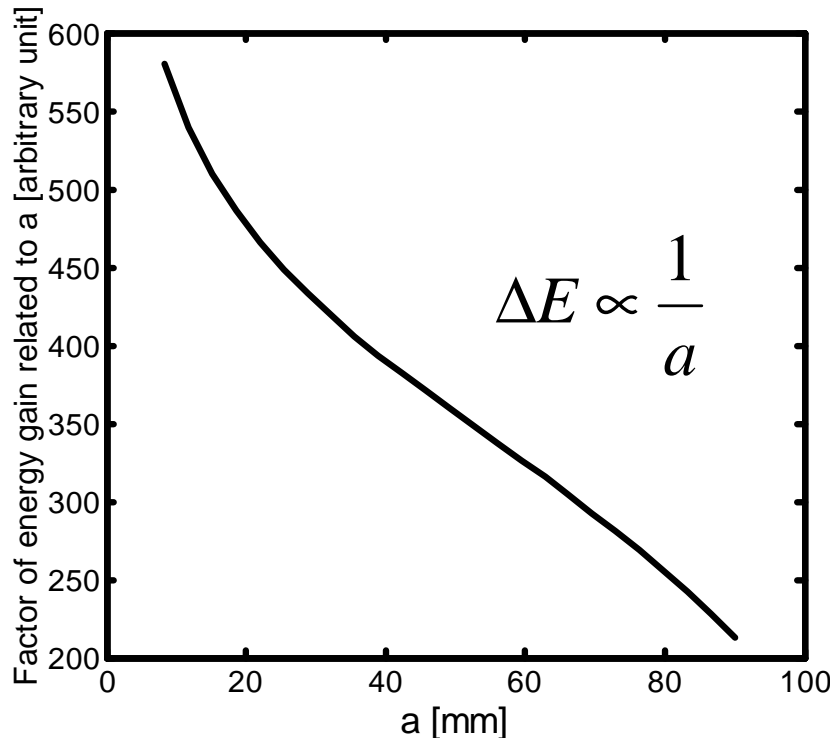


Motion of a charged particle in the earth's magnetic field

Transverse Beam Size Effects

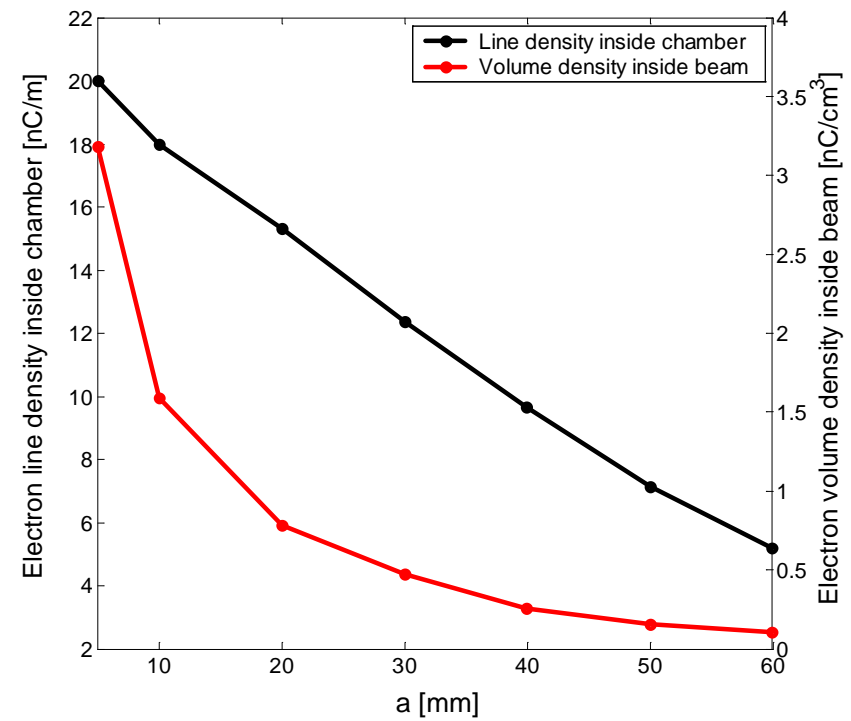


- A smaller beam size contributes to stronger space charge field and hence larger electron energy gain and stronger multipacting.
- Instabilities is sensitive to a . Small a , strong instability



$$\lambda_{chamber}[nC/m] = 21 - 0.27a[\text{mm}]$$

$$\rho_{cen}[nC/cm^3] = 4.9e^{-0.1a[\text{mm}]}$$



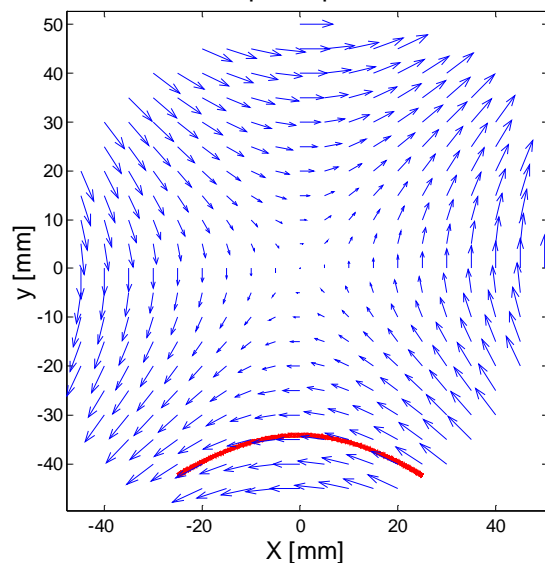
Orbit of the Guiding Center



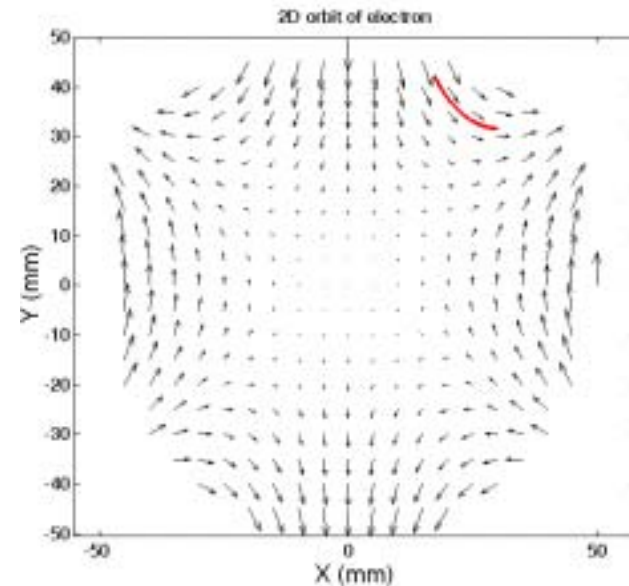
Orbit of Guiding Center

$$\mathbf{A}^* = \mathbf{A} + \frac{m\mathcal{V}_\parallel}{eB} \mathbf{B} = \text{const.} \quad \text{for general fields}$$

$A_z = \text{const.}$ for translationally symmetric quadrupole & sextupole fields



$$A_z = A_2(x^2 - y^2)$$



$$A_z = A_3(x^3 - 3xy^2)$$